Diploma thesis

The significance of skin microbiome in the pathophysiology of polymorphic light eruption

submitted by

Maximilian Zarfl

in partial fulfillment of the requirements for the degree of

Doktor(in) der gesamten Heilkunde

(Dr.(in) med. univ.)

at the

Medical University of Graz

executed at the

Departement of Dermatology and Venerology

supervised by

Univ. Prof. Dr. med. univ. Peter Wolf

Dr.in rer. nat. Natalie Bordag

Vijaykumar Patra, MSc. PhD

Graz, 20.07.23

Affidavit

I solemnly declare that I have independently and without any external assistance authored the present work, that I have not used sources other than those indicated, and that I have clearly indicated any passages taken directly or indirectly from the used sources.

Graz, 20.07.2023 Maximilian Zarfl eh.

Acknowledgements

I would like to express my deepest gratitude to Univ.-Prof. Dr. Peter Wolf, whose unwavering guidance, support, and encouragement have been instrumental in the successful completion of this research project. His profound knowledge and keen insight have significantly contributed to the quality of this work, and I am truly grateful for his dedication and patience, throughout the entire process.

I would also like to extend my heartfelt appreciation to Dr.in Natalie Bordag, Vijaykumar Patra, MSc, PhD, Dr. Franz Quehenberger, MSc. Isabella Perchthaler, Gerlinde Mayer, Dr.in Nicole Golob-Schwarzl, Prof. Dr. Lorenzo Cerroni, Dr.in Romana Kupser, Dr. Harald Köfeler, Dr.in Birgit Gallé, whose invaluable support and assistance played a crucial role in the development of this research.

To all these important contributors, I offer my sincere thanks for making this project a fruitful and rewarding experience. Your collective expertise and mentorship have undoubtedly enriched my understanding and have left a profound mark on my intellectual journey.

Finally, I want to thank my family for extraordinary support in challenging situations.

Inhaltsverzeichnis

Abbreviations

AMP	antimicrobial peptides
ANOSIM	analysis of similarities
ANOVA	analysis of variance
AXIN1	axis inhibition protein 1
CCL	C-C motif chemokine ligand
CSF1	colony-stimulating factor 1
CTRL	control subjects (healthy subjects)
CTRLs	control group (plural form)
CXCL	C-X-C motif chemokine ligand
DNA	deoxyribonucleic acid
DNER	delta and notch-like epidermal growth factor-related receptor
4EBP1	eukaryotic translation initiation factor 4E-binding protein 1
FDR	false discovery rate
Flt3L	fms-like tyrosine kinase 3 ligand
FOXP3	forkhead box protein P3
H&E	hematoxylin and eosin
HGF	hepatocyte growth factor
HPLC	high performance liquid chromatography
HWR	hip-to-waist ratio
IL	interleukin
LOG2LME	log2 linear mixed-effects
LOD	limit of detection
MCP	monocyte chemoattractant protein
MED	minimal erythema dose
MiRKAT	microbiome regression-based kernel association test
NMDS	non-metric multidimensional scaling
NPX	normalized protein expression
NaCl	sodium chloride
NIH	national institutes of health
Oct	octeniderm
PCR	polymerase chain reaction

PCA	principal component analysis
PLSDA	partial least squares discriminant analysis
PLE	polymorphic light eruption
PERMANOVA	permutational multivariate analysis of variance
ROC	receiver operator curve
RNA	ribonucleic acid
SEM	standard error of mean
SIRT2	sirtuin 2
SNPs	single nucleotide polymorphisms
ST1A1	sulfotransferase family 1A member 1
STAMPB	six transmembrane protein of prostate 2
SSUVR	solar-simulated ultraviolet radiation
TWEAK	tumor necrosis factor-like weak inducer of apoptosis
TNF	tumor necrosis factor
TNFα	tumor necrosis factor alpha
TNFSF4	tumor necrosis factor superfamily member 4
TLR5	toll-like receptor 5
TRAIL	tumor necrosis factor-related apoptosis-inducing ligand
Tregs	regulatory T cells
UCA	urocanic acid
UVA	ultraviolet A
UVB	ultraviolet B
UVR	ultraviolet radiation

List of figures

List of tables

Zusammenfassung

Hintergrund: Die polymorphe Lichtdermatose (PLD) ist die häufigste Photodermatose und verursacht im Frühjahr/Frühsommer Episoden von Hautanomalien, die mit saisonalen Veränderungen in der Suszeptibilität zur UV-induzierten Immunsuppression in Verbindung gebracht werden. Obwohl die Pathogenese nicht vollständig verstanden ist, bestehen evidente Hinweise, dass das Hautmikrobiom eine entscheidende Rolle spielen könnte. Präklinische Daten haben gezeigt, dass das Hautmikrobiom die UV-induzierte Zytokinexpression regulieren und die nachfolgende Immunantwort modulieren kann.

Zielsetzung: Das Ziel der Studie war es, die Wirkung der Hautdesinfektion bei Patient*innen mit polymorpher Lichtdermatose (PLD) zu untersuchen, um der Fragestellung nachzugehen, ob das Hautmikrobiom die Expression von Zytokinen beeinflusst und somit eine Rolle in der Pathophysiologie der Erkrankung nach sonnenlicht-simulierter UV-Exposition spielt.

Methoden: Es wurde eine randomisierte, placebo-kontrollierte, doppelblinde, Pilotstudie durchgeführt, an der 6 Patient*innen mit PLD und 15 gesunde Kontrollproband*innen teilnahmen. Es wurden ein Test zur Bestimmung der minimalen erythematösen Dosis (MED) und Photoprovokationen, sowohl an desinfizierter als auch nicht-desinfizierter Haut, durchgeführt. Ferner wurden Zytokine aus Saugblasenflüssigkeit (mittels OLINK 96 Target Inflammation Panel) - analysiert, sowie Hautabstriche und Klebestreifen für die Mikrobiomanalyse und die Analyse von cis-Urocaninsäure (cis-UCA) abgenommen. Zusätzlich wurden Hautbiopsien entnommen, um intra- und interindividuelle Vergleiche von UV-exponierter, desinfizierter und nicht-desinfizierter Haut zu ermöglichen.

Ergebnisse: Insgesamt gab es keine signifikanten Unterschiede in den klinischen Endpunkten (Erythem und Pigmentierung) zwischen Patienten*innen mit PLD und Kontrollproband*innen (auch nicht zwischen desinfizierter und nicht desinfizierter Haut). Patient*innen mit PLD zeigten eine beeinträchtigte Zytokinproduktion in nicht-exponierter, unbehandelter Haut und UV-exponierter, nicht-desinfizierter Haut bei MED. Die Fähigkeit der Patient*innen mit PLD zur Zytokinproduktion wurde durch Desinfektion nach mehrfacher UV-Exposition wiederhergestellt.

Diskussion: Ein reguläres Muster der Zytokinexpression wurde nach mehrfacher UV-Exposition und Desinfektion der Haut von Patient*innen mit PLD beobachtet. Aufgrund der geringen Anzahl der in die Studie eingeschossener Patient*innen erlauben die Ergebnisse der klinischen Studienendpunkte jedoch keine sicheren Schlussfolgerungen hinsichtlich biologisch-klinischer Relevanz der Hautdesinfektion bei PLD.

Schlussfolgerung: Patient*innen mit PLD zeigen eine beeinträchtigte Expression zahlreicher Zytokine und Chemokine, unabhängig davon, ob sie UV-Strahlung ausgesetzt sind oder nicht. Dies könnte für die UV-induzierte Immunsuppression mitverantwortlich sein. Desinfektion der Haut hat das Potenzial, die Produktion von Zytokinen bei Patient*innen mit PLD zu verbessern und die Dysbalance aufzuheben.

Abstract

Background: Polymorphic light eruption (PLE) is the most common photodermatosis, causing episodes of skin abnormalities in spring/early summer, which are associated with seasonal changes in susceptibility to UV-induced immunosuppression. Although the pathogenesis is not fully understood, there is evidence that the skin microbiome could play a crucial role. Preclinical data have shown that the skin microbiome can regulate UV-induced cytokine expression and modulate the subsequent immune response.

Aim: The aim of the study was to investigate the effect of skin disinfection in patients with polymorphic light eruption (PLE), to explore whether the skin microbiome influences the expression of cytokines and thus plays a role in the pathophysiology of the disease after sunlight-simulated UV exposure.

Methods: A randomized, placebo-controlled, double-blind pilot study was conducted involving 6 patients with PLE and 15 healthy individuals as a control group. A test to determine the minimal erythematous dose (MED) and photoprovocations, both on disinfected and non-disinfected skin, were performed. Moreover, cytokines from suction blister fluid (analyzed by OLINK 96 Target Inflammation Panel), skin swabs and adhesive strips for microbiome analysis, and cis-urocanic acid (cis-UCA) analysis were collected. Additionally, skin biopsies were taken to enable intra- and interindividual comparisons of UV-exposed, disinfected, and non-disinfected skin.

Results: Overall, there were no significant differences in the clinical endpoints (erythema and pigmentation) between patients with PLE and control subjects (nor between disinfected and non-disinfected skin). Patients with PLE demonstrated impaired cytokine production in non-exposed, untreated skin, and UV-exposed, non-disinfected skin at MED. The ability of patients with PLE to produce cytokines was restored by disinfection after multiple UV exposures.

Discussion: A regular pattern of cytokine expression was observed after multiple UV exposures and disinfection of the skin in patients with PLE. However, due to the small number of patients enrolled in the study, the results of the clinical study endpoints do not

allow for definitive conclusions regarding the biological-clinical relevance of skin disinfection in PLE.

Conclusion: Patients with PLE demonstrate impaired expression of numerous cytokines and chemokines, regardless of whether they are exposed to UV radiation or not. This could be partially responsible for UV-induced immunosuppression. Skin disinfection has the potential to restore cytokine production in patients with PLE and to correct the imbalance.

1. Introduction

Research in photoimmunology has unambiguously established the profound influence of ultraviolet radiation (UVR) exposure on the skin's immune system, manifesting in both localized and systemic immunosuppressive responses (1). This duality of UVR's immunosuppressive action is intriguing; on one hand, it is a significant predisposing factor to skin carcinogenesis, while on the other, its deficiency may precipitate certain autoimmune disorders, such as photodermatoses, including polymorphic light eruption (PLE) (2–4).

Furthermore, UVR exhibits a potent capacity for catalyzing photochemical reactions, leading to the modification of skin proteins and other molecular constituents (1). This results in the generation of altered or novel antigens, capable of eliciting immune responses (3). Thus, the immunosuppression induced by UVR could be conceptualized as an evolved biological strategy to mitigate the risk of autoimmune reactions in sun-exposed skin (3).

In recent years, substantial advances have been made in delineating the cellular components of the adaptive immune response and understanding the alterations following UV exposure (3). The spotlight has particularly been on regulatory T cells, a subset of T cells, whose role has been found to be indispensable in the context of UV-induced immunosuppression (5).

The potential effect of UV radiation exposure on the immune response through modulation of the skin microbiome is another dimension that warrants further investigation (6,7). The term "microbiome" encompasses the diverse microorganisms that cohabit an organism, with a dominant focus on gut bacteria but also extending to those residing on the skin (8). The composition of the skin microbiome is a dynamic entity, subject to variations based on the body location and interplays with the immune status (9).

Emerging evidence suggests that environmental influences, such as UV radiation, can induce shifts in the skin microbiome composition, thereby playing a pivotal role in maintaining cutaneous health and significantly impacting the trajectory of various skin disorders, including PLE (10).

1.1 Demographical and clinical aspects of PLE

Polymorphic light eruption (PLE) stands as the most prevalent entity among UV-inducible dermatoses, impacting approximately 18% of Europeans (11). The disease typically manifests between the 2nd and 3rd decades of life and exhibits a clear predisposition for women (3,12).

Patients with PLE characteristically present with intensely itchy, non-scarring, self-resolving skin lesions following substantial sun exposure, primarily in spring/early summer, during winter vacations in sunlit regions or exposure to artificial UVR (3,13). The lesions may manifest as erythematous macules, papules, vesicles, plaques, erythema multiforme-like lesions, or acneiform lesions, and generally maintain a monomorphic appearance within an individual (3,14). Commonly affected areas include the neck, V area, and upper arms, as these regions are infrequently exposed to sunlight during the cold season, leading to a loss of immunological adaptation to UVR, unlike the consistently UV-exposed facial skin (3).
Affected individuals often experience limitations in their daily activities, social interactions, and emotional well-being due to the persistent nature of the condition. The burden of the disease and the impairment of quality of life in patients with PLE are significant factors that correlate with higher risk of psychological comorbidities (15,16).

1.2 What's known in pathogenesis of polymorphic light eruption

Despite the wide prevalence of PLE its etiology remains largely elusive. Various pathogenetic models have been established, highlighting key mechanisms that play pivotal roles in the pathophysiology of the condition.
PLE appears to cluster in families: it has been estimated that a positive family history of PLE in first-degree relatives was present in 12% of affected twin pairs respect to 4% of unaffected twin pairs ($p < 0.0001$) (17). The probandwise concordance in monozygotic twin pairs was superior than in dizygotic twin pairs (0.72 vs. 0.30, respectively), demonstrating a strong genetic effect (17). According to a segregation analysis, it has been estimated that 72% of the UK population carry a low penetrance PLE susceptibility allele (18). Additionally, associations to certain HLA subtypes, such as HLA A24 and Cw4, were found to correlate positive with PLE (18). Despite the clear indications of genetic predisposition, studies that investigated specific gene alterations in PLE have yielded relatively few successes so far. However, one study has identified a high frequency of functional single nucleotide polymorphisms (SNPs) in NOD-2 and Toll-like receptor 5 (TLR-5) genes in patients with PLE (19). NOD-2, an intracellular pattern recognition receptor, and TLR-5, a cell surface receptor, both play a crucial role in recognizing specific microbial components and initiating immune responses (20,21). These findings are particularly intriguing given the established role of these genes in another skin condition, acute graft versus host disease (aGvHD), which is known for its immune-mediated damage to the skin upon UVR exposure (22). There

appear to be parallels in the response of Langerhans cells (LCs) to UVB exposure in both PLE and aGvHD (19).

In PLE, predominantly the ultraviolet A (UVA) spectrum (also UVA + UVB or UVB only) is recognized as a primary trigger of skin eruptions (12). One of the most prominent theories revolves around the concept that PLE patients exhibit as a delayed-type hypersensitive reaction to certain endogenous or exogenous antigens triggered by UV exposure(3). The nature of these antigens remains uncertain; however, they may derive from altered skin proteins or even components of the skin microbiota (23).

Another key mechanism that has been suggested involves a resistance to UV-induced immunosuppression (24). In UV-exposed PLE skin, reduced chemoattractant expression contributes to insufficient neutrophilic cell infiltration, and Langerhans cells (LCs) fail to adhere to their physiological migration pattern towards draining lymph nodes, which they usually do upon an UVR trigger (3,12,25). Neutrophil-derived TNF-α, IL-4, and IL-10 production and release are aberrant in comparison to healthy subjects (13). Additionally, there is inhibited mast cell infiltration (26). Mast cell-derived IL-10 facilitates the recruitment of $CD4^+$, $CD25^+$, $FoxP3^+$ Tregs, playing a vital role in immune tolerance (27). A functional defect in Tregs' capacity to induce regulatory T cell proliferation, accompanied by decreased FOXP3 mRNA, has been observed in PLE skin (28). Furthermore, the disease pathogenesis and recurrence are thought to be linked to enhanced accumulation of cytotoxic skin resident memory T cells (29).

1.3 Potential involvement of the skin microbiota in polymorphic light eruption

Besides the abnormal skin sensitivity to UVR, substantial evidence exists, indicating that the skin microbiome plays a role PLE and might contribute to failure in UVR-induced immune suppression (10,30).

UVR has the ability to exert a modulatory influence on the skin microbiome (7). This dynamic interaction between UVR and the skin microbiome can result in alterations in the composition of the microbial community and possibly disrupt the intricate balance of signaling molecules or lead to formation of microbial elements that drive inflammation (31). Such signaling molecules may encompass the range of antimicrobial peptides (AMPs) found in the skin. AMPs are effector molecules of the immune system with antimicrobial properties, playing a crucial role in defending against microorganisms on the skin and mucous membranes (32). AMPs exhibit broad-spectrum activity against gram-positive and

gram-negative bacteria, as well as viruses, fungi, and parasites (33). Some of these antimicrobial peptides contribute to the regulation of various cutaneous microorganisms and directly or indirectly affect immune cell crosstalk (34,35). In PLE, a distinct profile of AMPs is orchestrated after photoprovocation, which could potentially induce the differentiation of specific T cell subtypes driving the pathophysiological cascade (35).
Moreover, preclinical studies involving mice have demonstrated that UVB-exposed mice with a microbiome exhibit more pronounced inflammatory responses after contact sensitization compared to germ-free mice (36).

1.4 Aim of study

The present research project will investigate the extent to which the skin microbiome is relevant to the formation of an immune response and its suppression after UV exposure. The main assumption of this proof-of-concept study is that skin disinfection prior an exposure to UVR leads to a quantitative and qualitative change of physiological and pathological skin reactions in patients with PLE. Furthermore, the secondary hypothesis is that alteration of skin microbiome through direct damage to microorganisms on the skin surface and/or by changing the immune status of the skin modulates cytokine production and the transcriptional signature of the underlying immune response.

2. Materials and methods

2.1 Study design

The trial design was a prospective, randomized, double-blind, placebo-controlled, half-body, pilot study with 6 PLE patients and 15 healthy volunteers assigned in parallel. The study protocol (application number: 33-196 ex 20/21) was approved in March 2021 by the local ethics committee of the Medical University of Graz, Austria, according to the principles of the Declaration of Helsinki. To ensure transparency and provide detailed information about this pilot study to the public, an entry in CinlicalTrials.gov, a registry of the National Institutes of Health (NIH) was made (identifier: NCT04985526). All study procedures were performed between April 2021 and May 2021 at the Photodermatology Research Unit, Medical University of Graz, Austria.

2.1.1 Primary hypothesis

Removal of the skin microbiome by disinfection results in a reduced UV sensitivity with reduced expression of PLE-specific skin lesions measured by PLE-Score.

2.1.2 Primary endpoint

To compare photoprovoked, disinfected/non-disinfected PLE skin, a validated PLE-Score established by Gruber-Wackernagel et al., was used to evaluate key properties of PLE lesions(37). The primary endpoint is limited to the PLE group and does not allow a comparison with healthy subjects.

2.1.3 Secondary endpoints

In contradiction, secondary endpoints allow the intra-individual and group comparison of untreated, unexposed skin and disinfected/non-disinfected, UV-exposed skin. Those endpoints include comparison of erythema/pigmentation index, skin barrier function (trans epidermal waterloss), levels of cytokines and chemokines, cis-UCA concentration levels, bacterial DNA and microbial abundance, and transcriptomes. Another secondary endpoint specific to PLE is a histopathological comparison of photoprovoked disinfected and non-disinfected skin.

2.1.4 Inclusion/Exclusion criteria

General eligibility for a participation in the trial was limited to individuals aged 18 to 75 years. Specific to PLE, participants must meet the inclusion criteria of a typical medical history of the disease and, preferably, a previously documented positive photoprovocation result and/or histologically confirmed skin lesions.

To ensure that participants do not have any underlying conditions or circumstances that could interfere with the study's results or their personal safety, the following exclusion criteria were defined: presence or history of malignant skin tumors; dysplastic melanocytic nevus syndrome; photosensitive diseases such as porphyria, chronic actinic dermatitis, xeroderma pigmentosum, basal cell nevus syndrome; autoimmune diseases such as lupus erythematosus or dermatomyositis; antinuclear antibodies (anti-dsDNA, anti- SS -A/Ro, anti- SS -B/La) before the start of the study; covid-19; systemic treatment with steroids and/or immunosuppressive drugs within 4 weeks; systemic treatment with antibiotics within 6 weeks; local treatment with antimicrobial agents in the area of the test field within 6 weeks; systemic treatment with drugs that could influence inflammatory responses within 2 weeks before the start of the study; allergy to adhesive strips an/or adhesive material; psychiatric disorders; pregnancy or breastfeeding; (foreseeable) Individuals who are unable or unlikely to comply with the study's requirements.

2.1.5 Group size calculation

The number of patients required for each group (n = 15) is based on the results of two preliminary studies by the Dermatology University Clinic, Graz, Austria (Ethics No. 14-058 dated 03/04, No. 19-129 dated 07/08) in PLE patients with near-identical phototesting settings for whom statistical planning was performed in collaboration with Dr. Franz Quehenberger from the Institute of Medical Information, Statistics and Documentation, Graz, Austria(37,38). As in the previous studies, the occurrence of the intensity of PLE skin abnormalities (PLE-Score) in the UV-exposed test fields and the occurrence of the intensity of erythema and pigmentation in the UV-exposed MED test fields with the corresponding control fields are compared in a half-body fashion, each using a paired, nonparametric analysis. A standard deviation of ±1 from the mean of the PLE score of the active treatment (disinfectant) /placebo treatment (saline 0.9%) was used to plan the number of cases (alpha: 0.05, power: 90%, t-test, drop-out rate: 7%), resulting in a number of 15 participants per group. An interims power calculation was performed after inclusion of 15 CTRL and 6 PLE patients with an alpha of 0.05, for clinically relevant PLE score reduction by 25%, 30%, or 50%, which achieved a power of 80%, 92% and 99%, respectively. Since a power of 80% was achieved, the study was accordingly terminated in May 2021. To achieve an adequate homogeneity within and between groups, PLE patients and healthy subjects were matched by sex and age (+/- 5 years).

2.1.6 Enrollment

Participating PLE patients were recruited after screening the database of the phototherapy outpatient clinic of the Department of Dermatology, Graz, Austria either by personal contact by the dermatologists of the phototherapy outpatient clinic or directly by mobile phone contact. Healthy subjects were invited to participate in the study primarily through social media groups. An expense and travel cost compensation were funded through third-party funds of the Department of Dermatology, Graz, Austria, for a completed participation in the study. The payment was executed by the reimbursement office of the department.

2.1.7 Skin disinfection and placebo treatment

In this study, Octeniderm® (Schuelke & Mayr GmbH, Austria), a skin disinfectant containing 1-Propanol, 2-Propanol, and Octenidindihydrochlorid, was compared to conventional sodium chloride (0.9%, Fresenius Kabi GmBH, Austria) as a control. Octeniderm® has a wide range of antimicrobial activity and can remain effective for up to

48 hours, as stated by the manufacturer. In contrast, sodium chloride is not expected nor reported to have any impact on the skin microbiome.

2.1.8 Randomization and blinding

The Institute for Medical Informatics, Statistics, and Documentation at the Medical University of Graz, Austria, provided randomization of two agents (disinfectant and placebo) to subjects' test areas through its Randomization Service for Multicenter Clinical Trials (Radomizer.at). Unique codes, consisting of P/K (P for patient, K for control, referring to the German term), consecutive number, test area indication, and visit number, were generated for pseudonymization purposes.

Blinding was ensured by the partnership pharmacy of the Medical University of Graz, with staff labeling the optically identical, sterile pipette vials with the corresponding identification codes (**Fehler! Verweisquelle konnte nicht gefunden werden.**). The investigators were granted access to the randomization list only after completion of all clinical procedures in both groups.

Figure 1 – Treatment-based randomization and blinding

Original photograph of the used glass vials labeled with identification codes that indicate the test field for application of agents (saline and Octeniderm®).

2.1.9 Application

To apply the agents to the skin of the subjects, 12 ml of either the commercial disinfectant or sodium chloride was dispensed into a pipette vial and applied to the test areas. To minimize the effects of the disinfectant's characteristic odor, participants and investigators covered their nasal vestibules with sterile nasal clips or swabs. To ensure consistent

application and slow evaporation, sterile cotton compresses (Gazin®, Lohmann & Rauscher GmbH & Co. KG, Austria) were soaked with the solution using a glass pipette attached to the top of each vial. The soaked compresses were left on the skin for 60 seconds, which is the recommended exposure time for the disinfectant. The treatments were applied 24 hours before SSUVR exposure and again immediately before to the exposure.

2.2 Phototesting

2.2.1 Light source

Several photo systems were tested and compared prior to the start of the study. In this study, the Waldmann UV 801 KL system was utilized for phototesting. The system was equipped with helium lamps from Helarium Wolff Systems (Arimed B40 light tubes, B1-12-40W/BIPIN). A comparison between the light spectrum generated by this system and the sun-simulated light of the system previously used in other studies to induce PLE is shown in (Figure 2) (37,38). Irradiance was routinely measured and monitored by a broad-band thermopile radiometer (Dexter Research 2M model with quartz window; Medical Physics, Dryburn Hospital, Durham, U.K.). The mean irradiance (290 - 400 nm) at skin level (at a distance of 15 cm to the outer- most filter of the light source) was 2,00 mW/ cm^2.

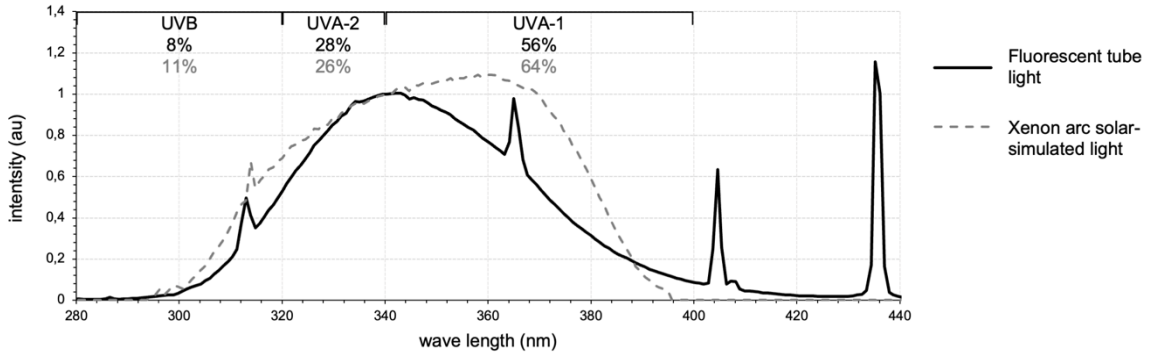

Figure 2 – Comparison of light source in this study to previous work

Intensities were normalized to 1 at 340 nm for simpler comparison and percentage of UVB, UVA-1 and UVA-2 emission from total spectrum is shown above the curves. The here used fluorescent tube light is similar to the Xenon arc solar-simulated light emission with a slightly lower UVB and slightly higher UVA-1 content.

2.2.2 MED testing

At visit 2, 24 hours after the initial UV exposure, subjects' individual MED was determined using a standardized MED protocol (**Fehler! Verweisquelle konnte nicht gefunden werden.**). Two ladders with 6 test fields 1.5 cm in diameter were placed horizontally on the upper back (**Fehler! Verweisquelle konnte nicht gefunden werden.**). The physical doses

for the MED were gradually increased by an increment factor of √2 from 0.71 mW/cm^2 (test field 1) to 4.00 mW/cm^2 (test field 6). Cotton textiles were used to protect the adjacent skin.

2.2.3 Photoprovocation

For the PLE group, four consecutive UV exposures were performed from visit 3 to visit 6. Two designated test fields, each 10 x 10 cm in size, were located above the MED area (**Fehler! Verweisquelle konnte nicht gefunden werden.**). Cotton textiles were again utilized to protect the adjacent skin. For the first photoprovocation, a dose equivalent to 75% of the individual MED was used, and the dose was increased by 0% to 25% for each subsequent UV exposure. If visible erythema was observed 24 hours after an exposure, the subsequent dose was maintained or depending on the erythema intensity even reduced by up to 25%.

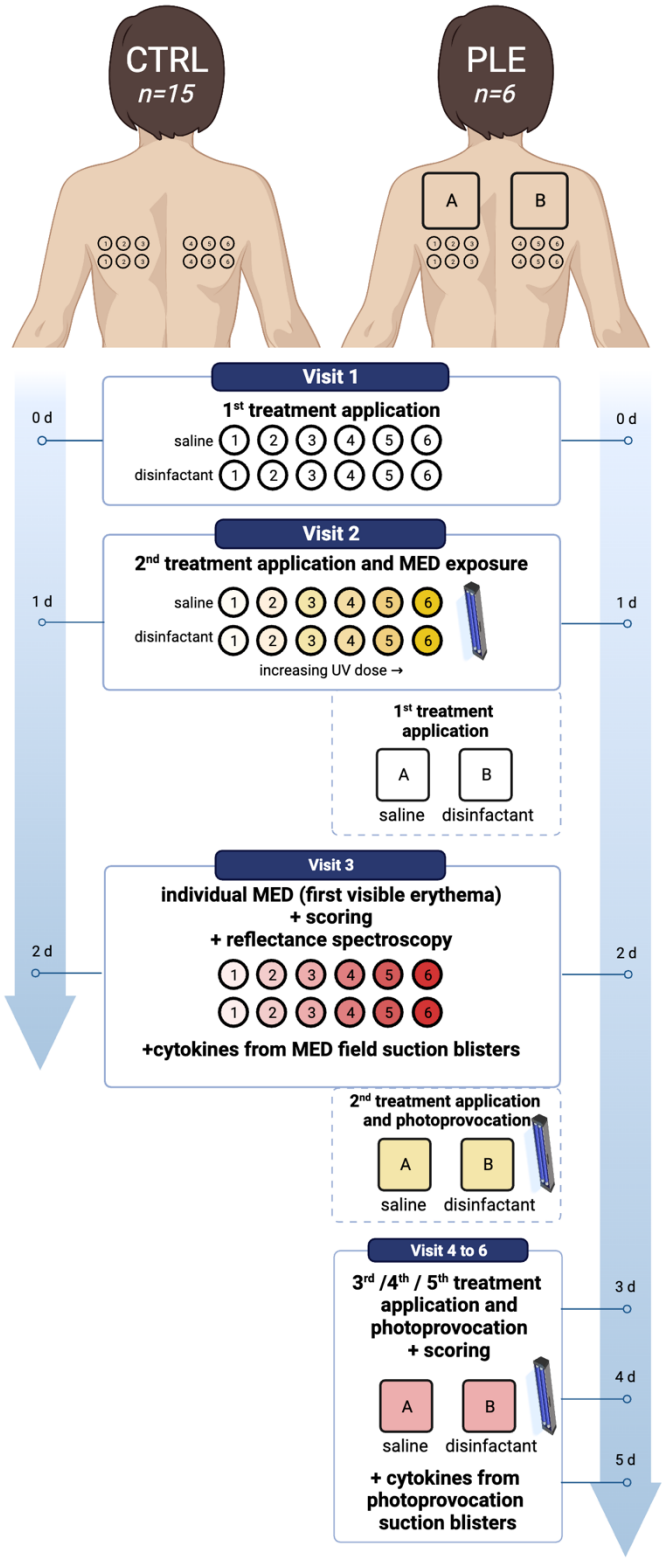

Figure 3 – Schematic illustration of the study protocol

Treatments (disinfectant and saline) were administered 24 hours before and immediately prior to each UV exposure. The MED was assessed at visit 3 (24 hours after MED exposure), followed by collection of blister fluid for cytokine analysis at the MED dose test field. In the PLE group, a mild photoprovocation was carried out with four mild UV exposures on consecutive days and blister fluid was collect at the last visit 6.

2.3 Clinical Evaluation

2.3.1 Assessment of skin type and hip-to-waist ratio (HWR)

At study day 0, certain individual properties such as skin type according to Fitzpatrick scale and HWR were determined. HWR was measured at the narrowest point of the waist, usually just above the belly button and the widest point around the buttocks.

2.3.2 Visual assessment of erythema and pigmentation

The MED is defined as a slight, homogenous erythema 24 hours after UV-exposure.

To assess the MED at visit 3, a validated numerical scale and scoring system was used to visually assess the intensity of erythema on a scale of 0 to 4 (Table 1) (37). Similar to Erythema-Scale, a Pigmentation-Score of 0 to 4 was used (Table 2).

Additionally, a qualitative parameter was established to compare and distinguish between more (">"), equal (" ="), or less ("<") of the physiological skin reactions in comparison. This was in particular useful when comparing test fields that made the same scale or points.

Table 1 – Erythema-Scale

SCALE	ERYTHEMA
0	no erythema
0.5	slight, inhomogeneous erythema
1	slight, homogeneous erythema
2	dark erythema
3	dark erythema with edema
4	dark erythema with blistering

Table 2 – Pigmentation-Score

POINTS	*PIGMENTATION*
0	none
1	slight
2	moderate
3	extensive
4	maximal

2.3.3 PLE-Score assessment

In the PLE group, a validated PLE score was also determined to evaluate photoprovocated skin symptoms, taking into account affected skin area, skin infiltration, and pruritus levels: AA + SI + 0.4P (range, 0 to 12); AA = affected skin area from 0 to 4 (0 = none, 1 = 1 to 24%, 2 = 25 to 49%, 3 = 50 to 75%, 4 = 75 to 100%); SI = skin infiltration from 0 to 4 (0 =

none, 1 = slight, 2 = moderate, 3 = extensive, 4 = maximum), P = pruritus on a visual analog scale from 0 to 10 (37).

2.3.4 Reflectance spectroscopy

To further quantify erythema and pigmentation, a reflectance spectroscopic instrument DSM II colorimeter (Cortex Technology, Hadsund, Denmark) was utilized to conduct colorimetric measurements of UV-exposed test fields from MED testing and control skin at visit 3. According to the user manual of the device at each study day the obligatory initial calibration on the white, clean calibration surface was performed. The values from erythema and melanin intensity based on triplicate measurements were averaged for each test field.

2.3.5 Skin barrier function determination

The measurement of transepidermal water loss (TEWL), a qualitative parameter of skin barrier function, was performed utilizing the Cutometer® Dual MPA 580 (Courage + Khazaka electronic GmbH, Cologne, Germany) with its TEWL probe. The completely painless and non-invasive examination involves placing the probe on the respective test area and taking triple measurements, each lasting approximately 3 to 5 seconds. The measured values are recorded by the compatible software running on Microsoft systems and are exportable directly to Microsoft Excel for further statistical analysis.

2.4 Cis-urocanic acid analysis

2.4.1 Tape strip method

Cis-UCA was determined from adhesive tape strip samples. To perform this method, transparent adhesive discs (Standard D100-Squame Standard Sampling Discs, CuDerm Corporation) 0.7 cm in diameter were used to collect *stratum conreum*-derived skin material. Samples were obtained from untreated, unexposed skin and after MED from disinfected and saline-treated skin at visit 3. According to the recommendations of the manufacturer, the first 3 discs were discarded, and the fourth and fifth disc were adhered a total of 20 times at constant pressure and velocity. This is suggested to remove most of the *stratum corneum* and allows determination of UCA and its isomers. The adhesive strips were immediately placed in sterile Eppendorf tubes and stored at -80°C until further processing.

2.4.2 High performance liquid chromatography

Urocanic acid (UCA) levels from tape strip material of PLE patients and healthy subjects were quantified using HPLC. The process of HPLC was done in cooperation with the Dr. Harald Köfeler, core facility mass spectrometry, Medical University of Graz, Austria.

Prior to analysis, the tape strip samples were homogenized using a Precellys®24 Homogenizer (Bertin Technologies, France) to ensure uniform distribution of the skin material. Following homogenization, the samples were subjected to an extraction procedure using a mixture of 0.1 M KOH, 1 M potassium hydroxide (KOH) and 25% (weight/weight) ammonia, which was specifically designed to extract Urocanic acid (UCA) (39).

To further isolate the UCA, samples were centrifuged at a velocity of 14,000 rpm for a duration of 15 minutes at a temperature of 4°C using an Eppendorf® 5415R centrifuge. Supernatants were subsequently collected and prepared for analysis.

High-performance liquid chromatography (HPLC) was employed for the quantification of cis-UCA within the collected supernatants. The HPLC system for this (Agilent 1260 Infinity II LC System, Agilent Technologies, Santa Clara, California, USA) was equipped with a reversed-phase column (Agilent Poroshell 120 EC-C18 C18) reversed-phase column. The mobile phase utilized for chromatographic separation was an isocratic elution with hydrochloric acid (4.3 mM), sodium octane-1-sulfonate (0.1 mM), and acetonitrile (2%). The flow rate was set at 0.4 ml/min, with an injection volume of 20 µl. Detection of cis-UCA was performed with a UV detector set at a wavelength of 263 nm.

Quantification of cis-UCA was achieved by comparing the peak area from the chromatogram to a standard curve. Data processing was carried out using the Agilent OpenLAB CDS ChemStation Edition software, with the cis-UCA levels being expressed as µM.

2.5 Microbiome analysis

2.5.1 Skin swabs

During the study, subjects were instructed not to use any skin care products (such as soap, shampoo, lotion, etc.) on their back. Skin microbiome samples were collected for bacterial DNA analysis using skin swabs (BBL Culture Swab and Transport Medium System, BD Diagnostics) from untreated skin and both disinfected and saline-treated skin 24 hours after each UV exposure. Skin swabs were taken from every MED test field and from both photoprovocation test fields at multiple locations. To improve biomass absorption, swabs were taken wet using a solution of 0.15 M NaCl and 0.1% Tween-20, filtered and prepared

in a dispensary. The shaft of the swabs was trimmed with sterile surgical scissors to fit into the tubes and avoid contamination. Finally, samples were stored at -80°C until analysis.

2.5.2 16S ribosomal RNA (rRNA) sequencing

The 16S rRNA sequencing was done in cooperation with the Dr.in Birgit Gallé, Core facility of the Medical University of Graz, Austria.

The extraction of bacterial DNA from skin swab samples was performed using the DNeasy Blood & Tissue Kit (Qiagen, Netherlands), according to the manufacturer's instructions. This kit employs a combination of chemical and physical lysis methods, followed by a silica-based DNA purification protocol, to ensure the extraction of high-quality bacterial DNA. The purified amplicons were then sequenced using two different kits on the Illumina HiSeq 3000 platform. For the sequencing of smaller genomes and amplicons, the MiSeq v2 Nano Kit (Illumina, San Diego, California, USA) was employed. For the sequencing of larger genomes, the MiSeq Reagent Kit v3 (600-cycle) (Illumina, San Diego, California, USA) was utilized. These kits provided a combination of short-read and long-read analysis, offering a comprehensive view of the microbial species present (40).

2.6 Suction blister method

2.6.1 Equipment and technique

Suction blisters were induced using a CE-certified suction pump (Vacu Aide 7314P-NE, Georg Egger GmbH). The machine was connected by a single tube with a diameter of 2 cm to a purpose-built metal distributor with six mounts. This unit allowed to attach infusions tubes with 0.7 cm diameter that were connected to custom-made autoclavable suction chambers made of Plexiglas for simultaneous blister formation at multiple body locations (Figure 4). A constant negative pressure of 200 to 300 mmHg was applied until blisters formed within 45 – 75 minutes detaching the epidermis its dermal-epidermal junction, which is significantly faster than reported (41). The blister formation sites were based on the clinical score, the MED test field, the corresponding test field in the ladder below or above, and the untreated skin on the subjects' upper back. For PLE patients, the location was set in the center of the respective test field and was executed at visit 3 (immediately after clinical scoring and collection of skin microbiome samples) and visit 6 (after the last UV-exposure). Depending on the variable size and number of suction blisters formed at a test site, a total volume of approximately 15 – 50 µl of blister fluid was aspirated with tuberculin syringes (Omnifix®-F, B.Braun GmbH, Austria). Samples were collected in 0.5 ml Eppendorf tubes

with flat seal caps (Thermo Fisher Scientific Inc., Waltham, Massachusetts, USA), diluted 1:1 with PBS, and stored at -80 °C until further work-up.

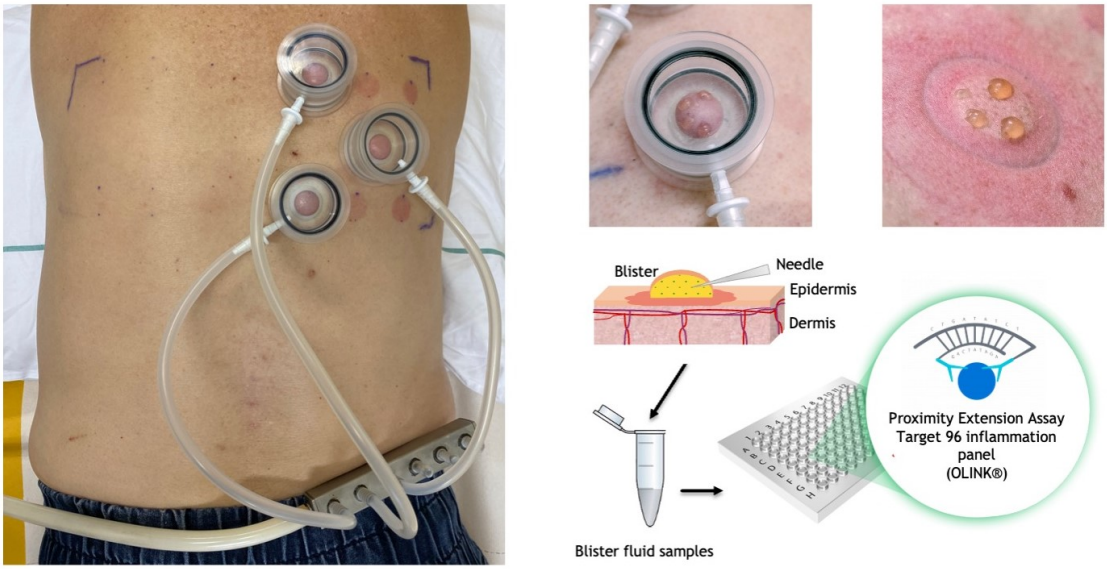

Figure 4 – Suction blister method for proteomic analysis

Photographs of the suction blister method on MED test fields and untreated, unexposed skin on the back of a healthy subject. The illustration shows the aspiration of blister fluid which has been made with a commercial tuberculin syringe. Obtained blister fluid got diluted with PBS 1:1 and stored at -80°C until shipment for multiplex proteomic analysis by OLINK® (Uppsala, Sweden).

2.6.2 Blister fluid analysis

Blister fluids were thawed in a water ice batch and protein concentration was determined with Bradford Assay (Biorad Protein Assay Dye Reagent, 500-0006; BioRad Laboratories GmbH, Munich, Germany) according to manufacturer's protocol. Blister fluids with concentrations above 10 µg/µl were diluted with PBS buffer to 10 µg/µl, all other 13 samples were kept undiluted, aliquoted into 96 well flat bottom plates, snap frozen on dry ice, stored at -80°C and shipped on dry ice for analysis.

Cytokine quantification was done by Olink® using their Target 96 Inflammation Panel, and performed at its facility in Uppsala, Sweden. Cytokine abundances are reported as normalized protein expression (NPX) values.

2.6.3 Blister roof sampling

The suction blister technique allowed the acquisition of the blister roof, comprising the detached epidermis, in addition to blister fluid aspiration. Samples were collected from multiple test sites of PLE patients and healthy subjects: unexposed and untreated skin;

disinfected and saline-treated MED skin; and disinfected and saline-treated photoprovoked skin.

Once a blister collapsed as a result of the blister fluid aspiration process, the blister roof was cut off with utmost care under aseptic conditions using sterile surgical instruments to prevent damage to the tissue and eliminate the risk of sample contamination and/or risk of skin infection. Following this minimal-invasive procedure, blister roof samples were immediately placed into autoclaved jars containing formalin and stored at -25°C to maintain tissue integrity. The samples were reserved for potential subsequent analyses, such as immunohistochemistry staining's. Hematoxylin and eosin (H&E) staining was performed analog to the punch biopsy samples described below (Figure 18).

2.5 Skin biopsies

Skin biopsies were performed by routined clinicians at the Universitätsklinik für Dermatologie und Venerologie, Graz on 3 PLE patients at visit 6, post-final UV exposure. Biopsies were obtained from disinfected and saline-treated, photoprovoked skin utilizing a sterile 4 mm punch biopsy instrument. Each procedure was conducted under local anesthesia with Xylanest® 1% under aseptic conditions. Punch biopsy tissue was immediately placed into formalin-filled jars and subsequently stored at -25°C until further processing by MSc. Isabella Perchthaler. Inter-individual histopathological comparison followed an initial standard protocol for hematoxylin and eosin (H&E) staining. First, formalin-fixed tissue was embedded in paraffin blocks. Subsequently, thin sections of 4 µm were prepared and mounted onto glass slides. Next, sections were deparaffinized and rehydrated through a graded series of alcohol solutions. Hematoxylin, a basic dye, was applied to stain the cell nuclei blue, while eosin, an acidic dye, was used to stain the cytoplasm and extracellular matrix in varying shades of pink.

Following the staining process, sections were dehydrated, cleared in xylene, and mounted with a coverslip for microscopic examination and imaging. Histopathological evaluation was performed by Prof. Dr. Lorenzo Cerroni and Prof. Dr. Peter Wolf.

2.6 Statistical analysis

2.6.1 Large language models

This work employed the combination of ChatGPT and InstaText.io as tools for improving the quality and coherence of the text. The generated output from these tools was then manually reviewed and checked for accuracy by the author.

2.6.2 PLE score, visual scores and absorption of erythema and pigmentation

For statistical analysis of treatment effect (saline vs. disinfection) upon UVR exposure paired t-test was utilized to compare the mean PLE scores, mean visual scores and mean absorption values of erythema and pigmentation. In this analysis, a significant treatment effect was determined when the p-value was equal to or less than 0.05. For visualization, dot plots were used to show group mean values and standard errors of the mean.

2.6.3 Cis-UCA data analysis

The cis-urocanic acid (cis-UCA) levels obtained from different skin conditions and analyzed by HPLC and subjected later to a two-way ANOVA statistical analysis using GraphPad Prism 9.

Before conducting the two-way ANOVA, data was examined for the assumptions of normality and homogeneity of variance. If these assumptions were violated, the non-parametric equivalent Kruskal-Wallis H test followed by post-hoc pairwise comparisons were used.

In the two-way ANOVA, the participant group (PLE/CTRL) and skin condition (disinfected/saline-treated UV-exposed skin and untreated, unexposed skin) were considered as independent variables. The dependent variable in this analysis was the level of cis-UCA. The test was conducted at a significance level of $\alpha = 0.05$, meaning that any p-value less than this threshold was considered to indicate a statistically significant difference. In case of a significant main effect or interaction, post hoc pairwise comparisons were performed using a Tukey HSD (Honestly Significant Difference) test to determine which skin condition differed from each other.

2.6.4 16S-sequencing data analysis

The bioinformatics analysis of the 16S rRNA sequencing data was conducted using a multi-step pipeline by Vijaykumar Patra, MSc, PhD.

Raw sequence data were initially processed using QIIME2 (Quantitative Insights Into Microbial Ecology), a powerful open-source bioinformatics pipeline (42). The processing involved quality filtering, error correction, and removal of chimeric sequences to ensure high-quality, reliable data for downstream analysis (42).

For alpha diversity analysis, which refers to the diversity within a particular sample or environment, various indices including observed species and Shannon index were computed. The differences in alpha diversity metrics between the different groups were statistically tested using the non-parametric Kruskal-Wallis test.

Beta diversity analysis, which assesses the diversity between different samples or environments, was conducted next. This involved the calculation of distance matrices using both unweighted and weighted UniFrac distances. These distances reflect the phylogenetic dissimilarities between the microbial communities in different samples. Non-Metric Multidimensional Scaling (NMDS) was used in beta-diversity analysis to visualize and compare the similarities or dissimilarities in microbial community composition between samples (CTRL baseline, PLE baseline, PLE photoprovoked).

Taxonomic analysis was conducted to identify the bacterial taxa present in the samples. The sequences were aligned against the SILVA reference database, a comprehensive database of curated 16S rRNA sequences, using the Nucleotide Basic Local Alignment Search Tool (BLASTn). The relative abundance of different bacterial taxa at various taxonomic levels (from phylum to species) was calculated.

All statistical analyses were performed with R v4.2.1 (43). The resulting data were visualized using various R packages, including 'ggplot2' for creating high-quality plots, and 'phyloseq' for microbiome analysis (44).

2.6.5 Proteomic data analysis

Data visualization and statistical analysis of the cytokine raw data were performed with R v4.2. using readxl, openxlsx, stringr, dplyr, tidyr, colorspace, RColorBrewer, ggplot2, ggpubr, nlme, emmeans, mixOmics packages) and TIBCO Spotfire v12.1.0, TIBCO, Palo Alto, CA by Dr. Natalie Bordag (43,45). Cytokine NPX values were normalized to total protein concentration and $\log_2$-transformed. Distribution and scedasticity were investigated with Kolmogorov–Smirnov test (*stats::ks.test()*) and Brown–Forsythe Levene-type test (*car::leveneTest()*), respectively. After $\log_2$-transformation of NPX values data was sufficiently normally distributed and homoscedastic, testing not significant with $p > 0.01$.

All 92 cytokine read-outs were evaluated based on percentage of data being within quantifiable range, above limit of detection (LOD) and below upper limit of quantification. In total, 21 cytokines were excluded from any analysis, 4 were suitable only for UVA (30%-50% outside quantifiable range) and 67 suitable for MVA & UVA (<30% outside quantifiable range). All samples with an initial total protein concentration of <5 µg/µl had to be excluded due to too high percentage of values below LOD (1 CTRL norm, 1 PLE norm, 1 PLE UV+Sal).

Only statistical methods were applied that can provide unbiased estimates for the here unbalanced group sizes pooled from independent experiments. Principal component analysis

(PCA) with 67 cytokines was performed centred, scaled, and multilevel to handle repeated measures of individuals with *mixOmics::pca(..., multilevel = "PatientID")*. The dataset contained no zeros and no missing values and since this was an exploratory study no multiple-test adjustments were applied.

Partial least-squares discriminant analysis (PLS-DA) with 67 cytokines was performed after imputation with *missMDA::imputePCA()* using 6 components. Analog to PCA PLS-DA was performed centred, scaled and with multilevel *mixOmics::plsda(..., multilevel = "PatientID")*. Significances of group differences were evaluated with *mixOmics::auroc()*. For univariate analysis of significant changes within each cytokine for the factor group (i.e. CTRL norm, CTRL UV+Sal, CTRL UV+Oct, PLE norm, PLE UV+Sal, PLE UV+Oct) linear models were fitted by maximum likelihood (ML) with *nlme::lme()* with random effect *~1|PatientID* to handle repeated measurements of individuals. For analysis LOG2 data was used, thus constituting it a non-linear approach which was abbreviated here with LOG2LME (log_2-transformed linear mixed models). Models with and without random factor were compared within each cytokine for lower AIC (Akaike information criterion; relative estimate of information loss), higher log-likelihood (goodness of fit), significance in log likelihood ratio test comparing, quality of Q-Q plots, randomness in residual and direct comparison of t-ratios. For 20 cytokines addition of the random factor significantly improved fit (Table 3) and had little impact in all other cytokines and the results from the models with random factor are reported throughout. Results of pairwise comparisons of interest were extracted with *emmeans::emmeans()*, without multiple test correction due to our exploratory approach.

The global null hypothesis that none of the cytokines were different between saline and disinfected skin after photoprovocation (visit 6) was subjected to the global test of Goeman et al (with R package globaltest) including the covariate PatientID as covariate because of the paired data structure (27), performed by Dr. Franz Quehenberger.

2.6.7 Signaling pathway enrichment analysis

To interpret the proteomic data in terms of biological functions, the STRING database (version 11.5) was utilized. The analysis included the UniProt IDs of the corresponding significantly altered cytokines from blister fluid analysis, along with their corresponding -log p-values in each comparison. The strength metric, calculated as the log10(observed/expected), was used to assess the magnitude of the enrichment effect. It represents the ratio of proteins in the analyzed network that are annotated with a specific

term to the number of proteins expected to be annotated with that term in a random network of the same size. The False Discovery Rate (FDR) was also considered to measure the significance of the enrichment, with p-values corrected for multiple testing within each category using the Benjamini–Hochberg procedure.

3. Results

3.1 Group homogeneity comparison

Comparative analyses of demographic and physiological parameters between PLE vs. CTRL demonstrated relative homogeneity. All study participants were of Caucasian descent. Fitzpatrick skin type, averaged across genders, was consistent across both groups (mean and median = skin type II). Age distribution exhibited minor discrepancies, with PLE males (n = 3, mean=29.00 years) and females (n = 3, mean = 24.33 years) slightly younger than their respective control counterparts (males: n = 7, mean = 27.00 years; females: n = 8, mean = 31.13 years). Notably, Waist to Hip Ratio (WHR), an indicator of metabolic health, differed between groups. While female PLE patients demonstrated lower mean WHR (0.750, low risk), male PLE patients had a higher mean WHR (0.991, moderate risk) compared to their respective control groups (females: 0.808, moderate risk; males: 0.892, low risk). A high HWR, indicating an increased risk of several health conditions, including cardiovascular disease, type 2 diabetes, and metabolic syndrome (46). In general, a healthy HWR for men is less than 0.9, and for women, less than 0.85 assuming measuring correctly.

3.2 UV response of disinfected and non-disinfected skin

The effect of UV exposure in PLE patients and CTRL on disinfected and saline-treated skin upon UV exposure was measured by reflectance spectroscopy and visually assessed. Both PLE patients and CTRL showed a dose-response relationship after UV exposure, confirming efficacy of the photo testing protocol (Figure 6). Pigmentation was very similar between PLE and CTRL ($p > 0.05$) prior to and after MED testing at all fields, irrespective of disinfection (Figure 6). Erythema absorption was also similar for PLE and CTRL before UV exposure and remained very similar in all MED test fields. Disinfection seemed to have no large impact on erythema, although at MED fields 2 and 6 only in PLE patients a weakly significant difference towards lower erythema in PLE was observed (Figure 6). Erythema and pigmentation scores were not impacted in PLE or CTRL by disinfection (Figure 5). In general, the MED testing increased erythema absorption with increasing dose as expected and had very little impact on pigmentation, so that the MED test was successful and safe.

The repeated mild photoprovocation stepwise increased parameters of the PLE score only slightly for affected area, infiltration and itch (Figure 7), indicating that the photoprovocation worked as intended and the here included PLE patients were rather mildly affected.

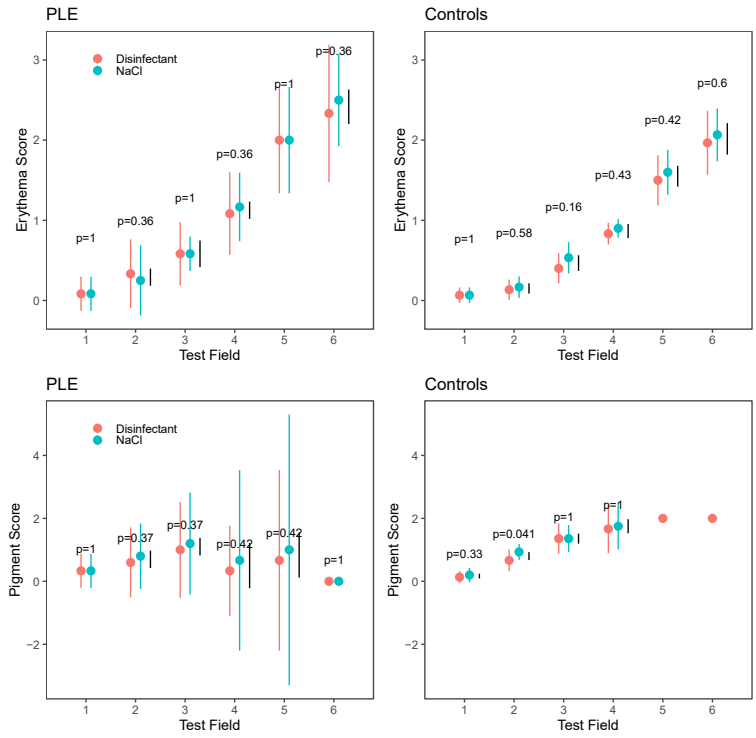

Figure 5 – Visual scores of erythema and pigmentation upon MED testing

Scores assessed by a validated numerical scale and scoring system (37). Dots represent the group mean of absorption values of treatment of each test field in PLE (n = 6) vs. CTRL (n = 15). Standard error of mean (SEM) is indicated as colored vertical line of each dot. The black vertical lines next to the dots of each test field indicate the distance required for a significant difference (p-value = 0.05) in treatment effect.

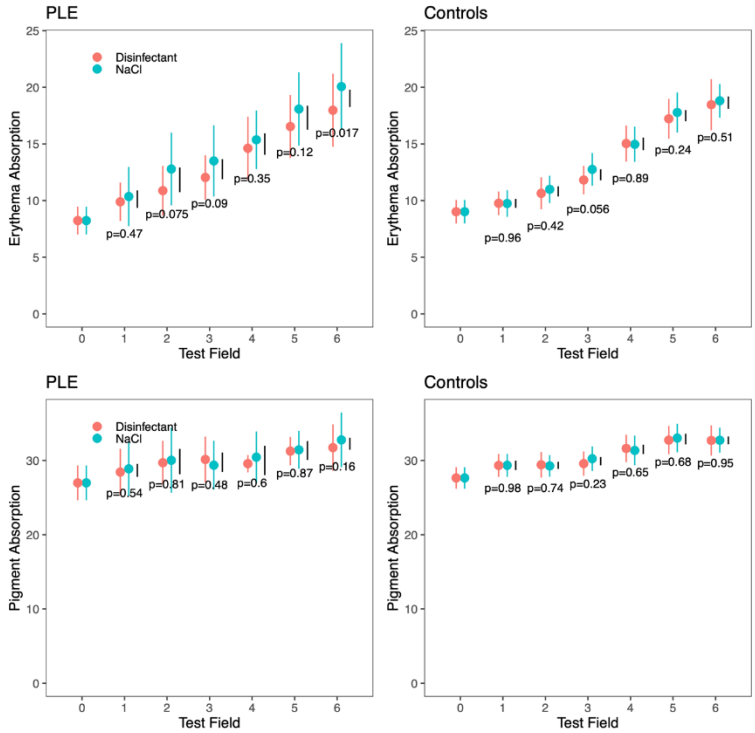

Figure 6 – Erythema and pigmentation absorption upon MED testing

Absorption of erythema and pigmentation was determined by reflectance spectroscopy. Dots represent the group mean of absorption values of treatment of each test field in PLE (n = 6) vs. CTRL (n = 15). Standard error of mean (SEM) is indicated as colored vertical line of each dot. The black vertical lines next to the dots of each test field indicate the distance required for a significant difference (p-value = 0.05) in treatment effect.

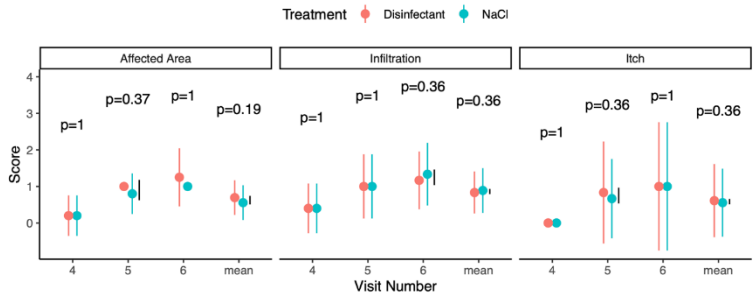

Figure 7 – PLE score results of photoprovoked skin

Dot plots of affected area, infiltration and itch, compromising PLE score, evaluated from visit 4 to visit 6 in six PLE patients at photoprovocated skin comparing saline (NaCL) vs. dsinfection. The standard error of mean (SEM) is indicated as vertical lines. The black vertical lines next to the dots of each test field indicate the distance required for a significant difference (p-value = 0.05) in treatment effect.

3.3 Cis-UCA production in PLE trend towards lower levels

Cis-urocanic acid (cis-UCA) is a small molecule found in the *stratum corneum* layer of the skin. It is formed from the amino acid histidine by photoisomerization triggered by the

exposure to UVB radiation. However, cis-UCA has been shown to suppress the immune response to UV radiation by inhibiting the production of cytokines and other immune signaling molecules that can help prevent inflammation and other harmful effects of UV radiation on the skin (1). To date, a cis-UCA analysis in patients with PLE in comparison to healthy subjects has not been made. Therefore, cis-UCA was determined from adhesive tape strip samples. The tape strip method is a minimal-invasive technique used in dermatology research to study the composition of superficial microbes, lipids/ceramides and superficially expressed proteins and peptides, such as UCA in the stratum corneum. The main objective of this analysis was to compare cis-UCA levels of patients with PLE vs. CTRL. Furthermore, intra-individual comparison and group comparison of cis-UCA levels in saline-treated skin vs. disinfected skin has been done to follow the hypothesis of a potential difference in cis-UCA levels in the context of absence or presence of the vast majority of skin microbes.

Analysis of cis-UCA levels using two-way ANOVA indicated diverging trends in PLE patients compared to healthy subjects (Figure 8). The Tukey HSD test controls for type I error rate, reducing the chance of false-positive findings that could arise when conducting multiple comparisons. Visual representation of the cis-UCA levels was achieved using dot plots (Figure 8). Control subjects, in line with our initial hypothesis, demonstrated increased cis-UCA levels after UV exposure on disinfected sites compared to saline-treated test fields exposed to similar UV doses (Figure 8). Contrarily, PLE patients showed an inverse tendency, with lower cis-UCA levels post-UV exposure on disinfected sites (Figure 8). However, comparing overall cis-UCA levels irrespective of treatment, PLE patients exhibited higher cis-UCA levels compared to CTRL (Figure 8).

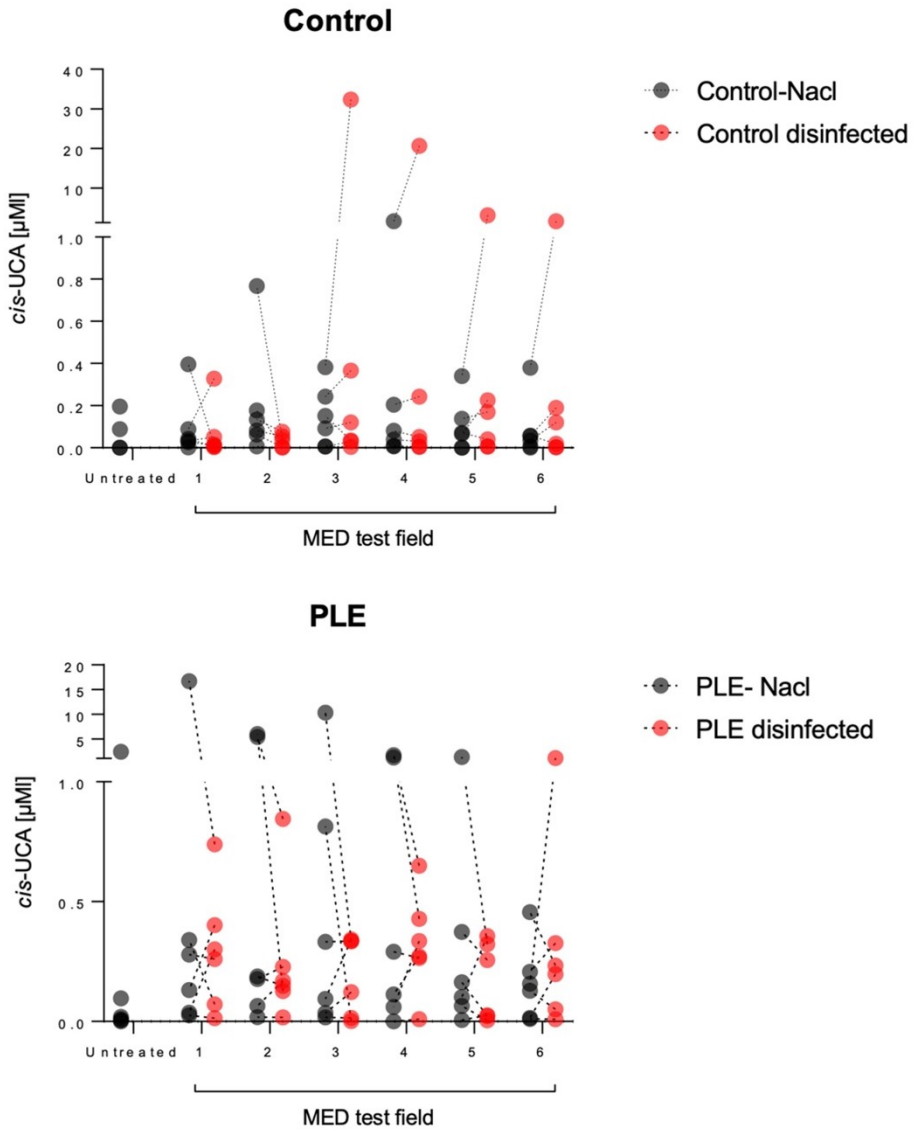

Figure 8 – Cis-UCA levels in PLE and CTRL

Each dot equals one individual and represent the mean of cis-UCA (measured per µM) in the respective treated MED test field (1 to 6) and untreated skin (baseline). Dashed lines connect dots of saline treated test fields (colored black) with dots of disinfected test fields (colored red) in PLE (n 0 6) and CTRL (n = 6) consistently.

3.4 Limited resolution of microbial abundance in PLE and CTRL

This pilot study aimed to achieve a detailed insight into the bacterial component of the skin microbiome in PLE patients in comparison to healthy subjects at baseline, and its potential changes in response to photoprovocation.

Skin swabs were collected from untreated, unexposed skin areas in both PLE patients and healthy subjects, as well as from disinfected and non-disinfected photoprovoked skin regions and subjected to 16S rRNA sequencing. 16S rRNA sequencing is a well-established method for characterizing the phylogeny and taxonomy of bacteria in complex microbial

communities. In dermatology research, this approach is typically utilized to investigate the bacterial domain of the skin microbiome, and to elucidate its role in skin health and disease (47).

However, due to limited number of reads of the skin microbiome samples obtained the comprehensive analysis was hindered (Figure 9). Considering an anticipated sample library size that would enable a feasible analysis of the skin microbiome, it is recommended to have read counts between 50,000 and 100,000 or higher (47). This range ensures a more robust and comprehensive assessment of the microbial composition and diversity to allow further interpretation. It is evident from the plot below that the majority of the samples from this study exhibited a very low number of reads (Figure 9). However, for the sake of learning and building a scaffold for follow-up studies a typical statistical analysis has been performed, although results are to be considered with utmost caution.

First, the alpha-diversity index of Shannon diversity and observed diversity was analyzed (Figure 10). Kruskal-Wallis test from nonparametric ANOVA analysis was performed and yielding a statistically significant result of Shannon diversity (p-value: 0.012092; Kruskal-Wallis statistic: 8.8304) and observed diversity (p-value: 0.024479; Kruskal-Wallis statistic: 7.4199). Those Kruskal-Wallis statistic values in conjunction with p-values below 0.05 suggest a large difference among the groups.

Second, beta-diversity was analyzed. Three different tests were conducted, including analysis of similarities (ANOSIM), permutational multivariate analysis of variance (PERMANOVA), and microbiome regression-based kernel association test (MiRKAT). However, none of the tests revealed any significant differences. For the ANOSIM test, the R statistic was -0.037109, with a p-value greater than 0.588. The R statistic is a measure of the dissimilarity between groups in the ANOSIM test. It ranges from -1 to 1, where values closer to 1 indicate greater dissimilarity between groups. The PERMANOVA analysis yielded an F-value of 1.2832 and an R-squared value of 0.10038, with a p-value of 0.224. The F-value is a statistical measure used in the PERMANOVA test and assesses the differences in group means by comparing the variability between groups with the variability within groups (48,49). Higher F-values suggest greater differences between groups. Additionally, the MiRKAT test showed an R-squared value of 0.017004 and a p-value of 0.69785, with a Kendall Rank Variance (KRV) of 0.0018946. In the MiRKAT (Microbiome Regression-Based Kernel Association Test) analysis, KRV measures the association between microbial composition and the factors of interest (disinfection vs. non-disinfection

= saline 0.9%) (50). A lower KRV value suggests weaker association between the factors and microbial composition. For visualization of beta-diversity, Non-Metric Multidimensional Scaling (NMDS) was used, a tool for dimension reduction, to compare the similarities or dissimilarities in microbial community composition between samples (CTRL baseline, PLE baseline, PLE photoprovoked) (51). As expected, microbial similarity is very similar between the groups (Figure 11). Taxonomy und phylogeny analysis reveal a limited view on the abundance of microbial composition in PLE and CTRL (Figure 12, Figure 13).

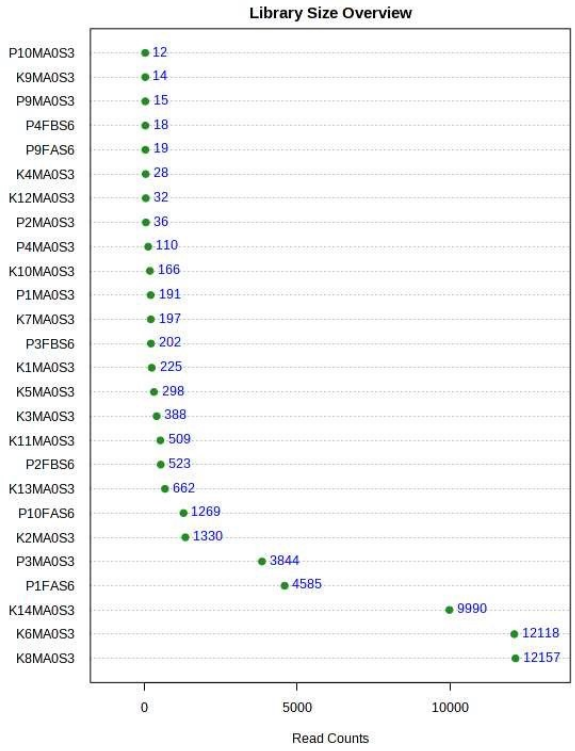

Figure 9 – Overall size of reads of 16S rRNA sequencing library

The x-axis represents the number of reads for each sample, while the y-axis denotes the different sample IDs from PLE patients (n = 6) and CTRL (n = 13) analyzed. Additionally, samples of photoprovoked skin in PLE (n = 6) were included to sequencing, resulting in a total of 12 samples.

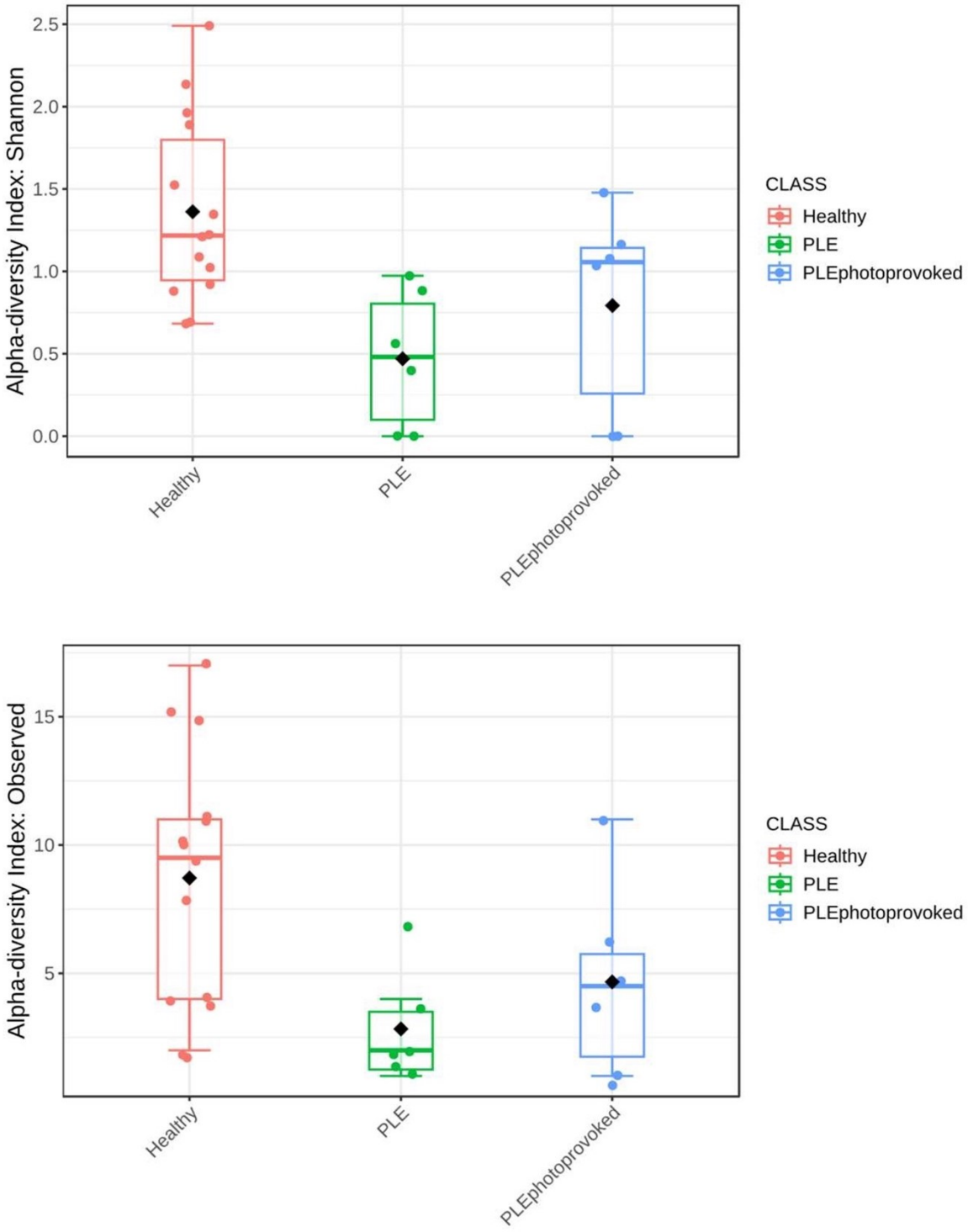

Figure 10 – Alpha-diversity analysis

Shannon (diversity): takes into account both the richness and evenness of the microbial community, calculating the entropy of the species distribution in a sample and considering the relative abundances of different taxa; Observed (diversity): measures the number of distinct taxa or operational taxonomic units (OTUs) present in a sample. It provides a count of the unique taxa without considering their relative abundances. Higher observed diversity values indicate a greater number of taxa or OTUs in the community.

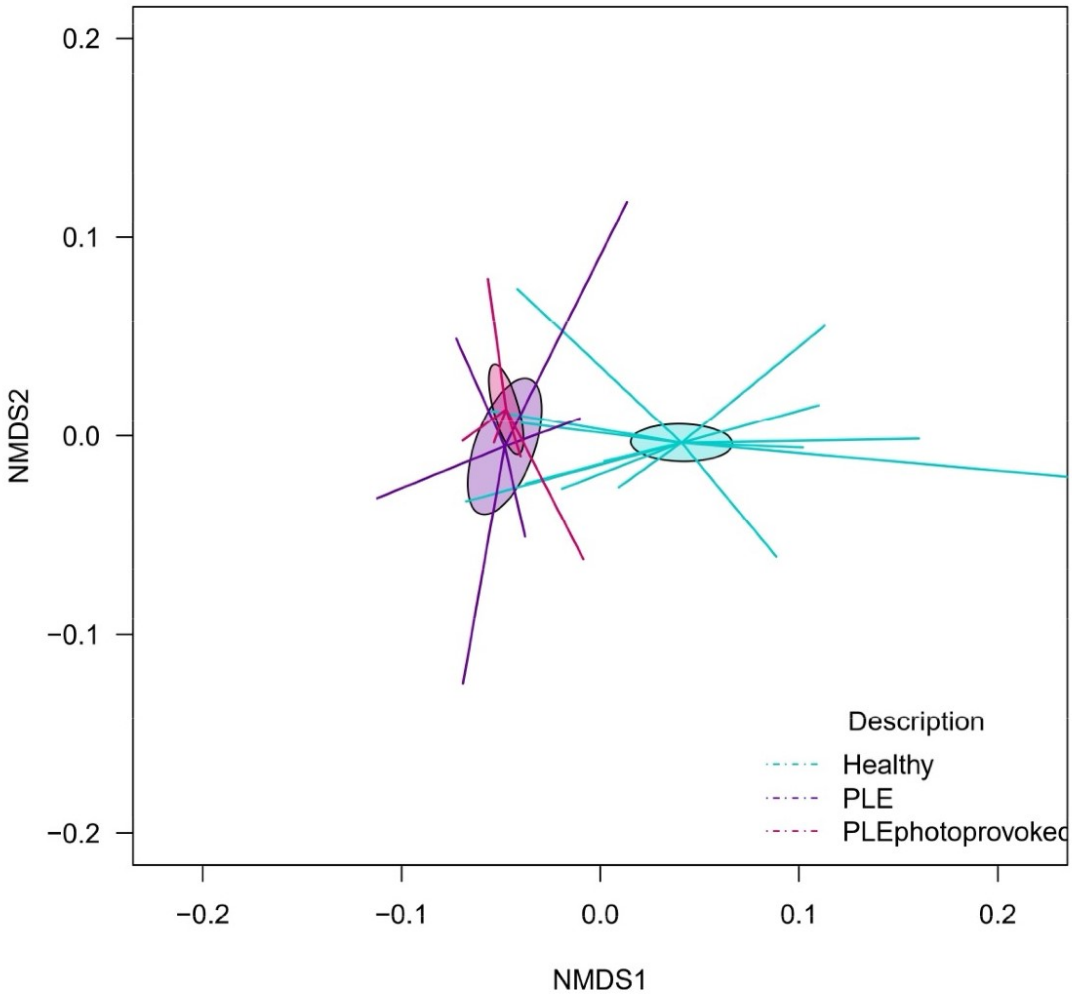

Figure 11 – NMDS plot of beta-diversity analysis

NMDS1 values, represented on the x-axis, explains the largest proportion of the variation in the data. It helps to separate samples that are most dissimilar in terms of their microbial community composition along this axis. NMDS2 values, represented on the y-axis, captures the additional variation that is not explained by the NMDS1 axis. It provides further separation and differentiation among samples along this axis, reflecting additional dissimilarities in their microbial community composition.

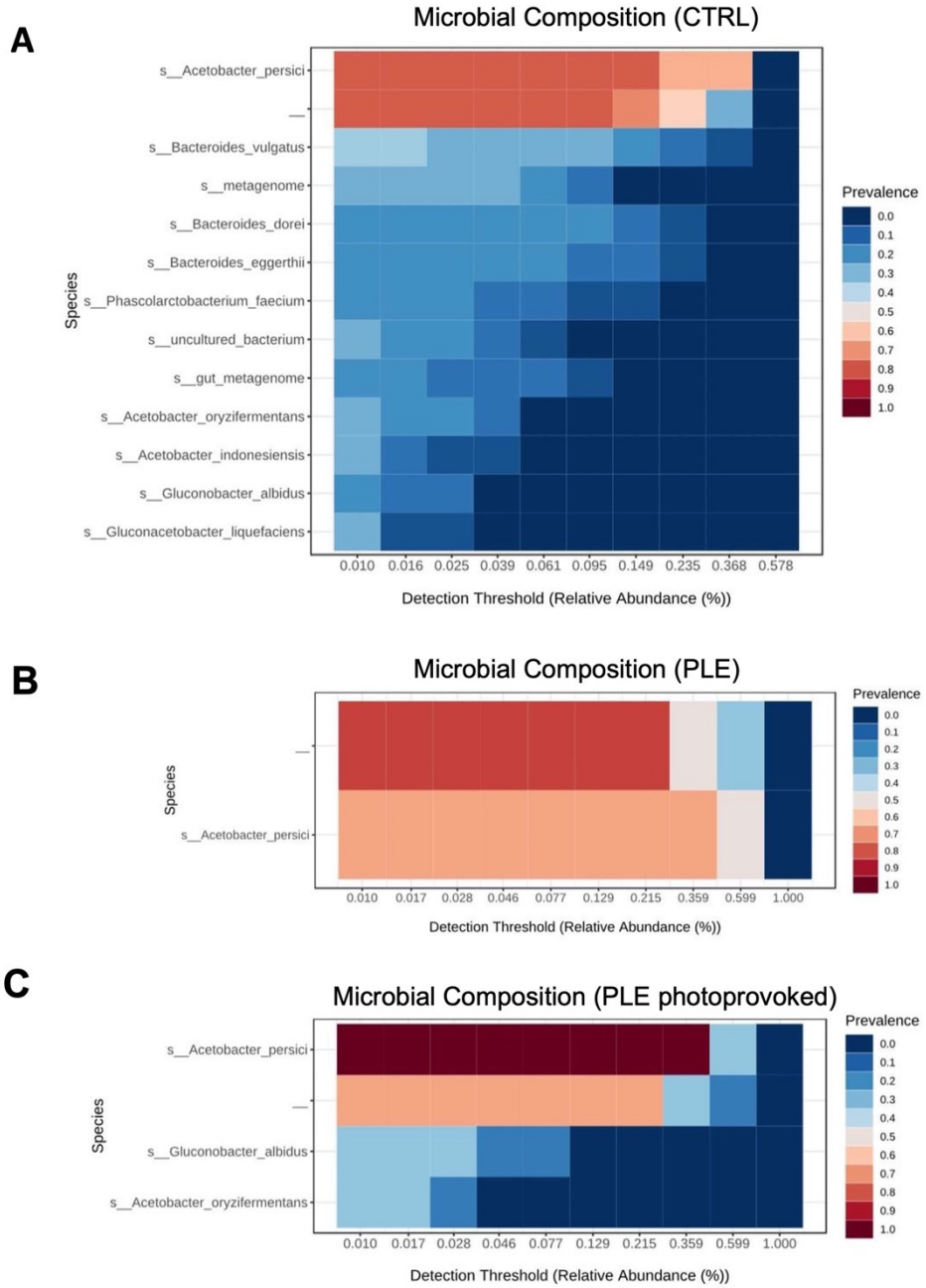

Figure 12 – Limited detection of microbial abundance in PLE and CTRL

In each heatmap, the y-axis represents the identified microbial species, while the x-axis represents the detection threshold expressed as relative abundance in percent. PLE patients (n = 6), CTRL; CTRL (n = 6).

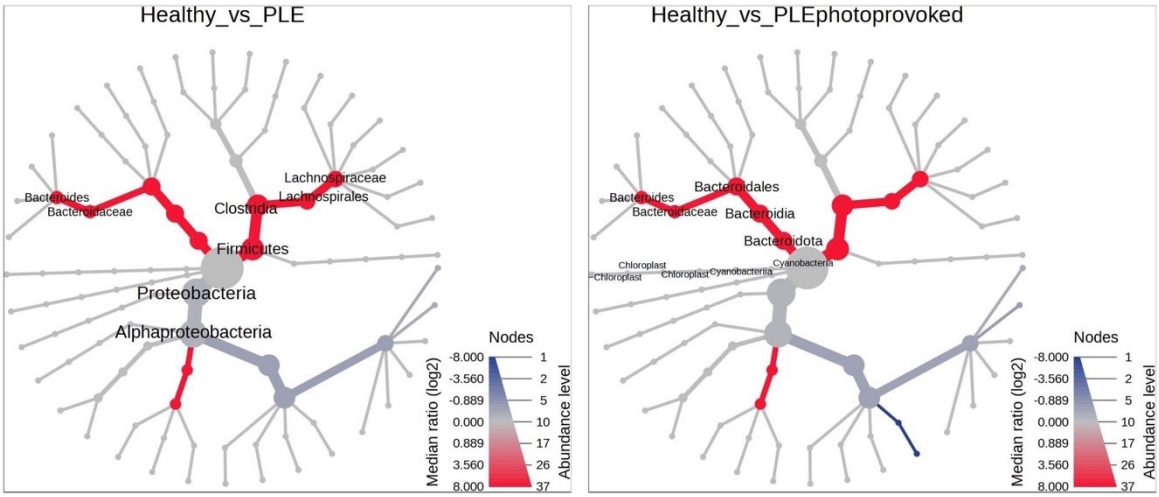

Figure 13 - Limited comparison of phylogenetics in PLE and CTRL

3.5 Impaired cytokine expression in PLE

The suction blister method is a widely used, minimally invasive technique in dermatological research for obtaining samples of the epidermis and dermis for proteomic and other molecular analyses. This method involves the artificial formation of suction blisters on the skin, allowing for the separation of the epidermal and dermal layers, which can be subsequently collected and analyzed. The method has been employed to study various skin disorders, including psoriasis, atopic dermatitis, and vitiligo, as well as skin aging and wound healing processes. The principle of the suction blister method relies on the application of negative pressure to the skin's surface, leading to the formation of a fluid-filled blister. The negative pressure induces a mechanical separation of the epidermis from the underlying dermis at the dermo-epidermal junction. Once the blister is formed, the roof of the blister (epidermis) can be carefully removed, and the blister fluid, containing various proteins and other molecules, can be collected.

Cytokine levels in freshly formed suction blisters were analyzed at visit 3 in unexposed skin and the MED test fields in both PLE and CTRLs, as well as at visit 6 in photoprovoked PLE skin (**Fehler! Verweisquelle konnte nicht gefunden werden.**, Figure 15, Figure 16). Using the Olink® target 96 inflammation panel, 72 different cytokines could be identified in blister fluid. Their proximity extension assay technology is based on artificial DNA-labelled antibody pairs that bind to a corresponding protein, hybridize in case of a match, and generate a signal for further amplification by PCR. (52,53)

Unbiased multivariate analysis with PCA found a slight trend towards differing cytokine levels after UV exposure (Figure 14A). The directed multivariate PLS-DA confirmed the weak, but significant impact of UV exposure on first response cytokine levels. An exploratory approach was used for a more detailed comparison of PLE vs. CTRL with linear mixed models (LOG2LME) without multiple test adjustment (Figure 14C). The cytokine levels were compared between PLE vs CTRL at the three different sites: unexposed, MED UV-exposed disinfected and UV-exposed saline (Figure 14B).

In unexposed skin PLE patients had lower immediate cytokine production for 20 cytokines (AXIN1, CCL11, CCL23, CSF-1, CX3CL1 CXCL6, DNER, Flt3L, HGF, IL-18, IL-33, Il-7, MCP-2, MCP-4, SIRT2, STAMPB, TNFSF4, TWEAK, TRAIL, 4EBP1 (Figure 15). After UV exposure PLE cytokine levels became more similar to CTRL, with only 11 cytokines being significantly lower in PLE, but with a less pronounced decrease than in unexposed skin (CSF-1, IL-1α, IL-10, IL-18, IL-33, MCP-4, SIRT2, STAMPB, TRAIL, 4EBP1) (Figure 15). Disinfection further reduced the cytokine level differences between PLE and CTRL remaining with only two sig. lower cytokine (CXCL11, ST1A1) (Figure 15).

A photoprovocation of four consecutive mild UV-exposures (starting dose = 75% of MED) were performed in PLE patients and suction blister samples were obtained immediately after the last UV-exposure (visit 6) in saline and disinfected skin. Both multivariate methods, the unsupervised PCA and the supervised PLS-DA found significant impact of disinfection on the patients' cytokine profiles after photoprovocation (Figure 16A, B). The global test, according to Goeman et al, for all cytokines confirmed that disinfection significantly affected cytokine production with $p = 0.0063$ (Figure 16C)(54). Accordingly, the LOG2LME univariate analysis showed that disinfection increased cytokine production notably and significantly for 45 cytokines (Figure 16D). Thus, the reduced capacity for cytokine production of PLE patients at baseline (unexposed skin) was rescued by disinfection during photoprovocation.

Table 3 – List of identified cytokines

	MED untreated skin (CTRL vs PLE)	MED saline-treated (CTRL vs PLE)	MED octeniderm-treated (CTRL vs PLE)	4x octeniderm-treated (PLE) SSUVR
Sign. Cytokines	*p-value* ***(< 0.05)***			
ADA	0,262	0,266	0,755	**0,009**
AXIN1	**0,022**	0,051	0,555	**0,001**
CASP-8	0,067	0,080	0,320	**0,030**
CCL11	**0,035**	0,137	0,466	**0,006**
CCL20#	0,928	0,132	0,934	**0,045**
CCL23#	**0,017**	0,056	0,616	**0,006**
CCL25	0,316	0,187	0,841	**0,005**
CCL3	0,136	0,325	0,591	**0,042**
CCL4	0,089	0,182	0,278	**0,046**
CD244	0,165	0,216	0,323	**0,008**
CD40	0,159	0,212	0,965	**0,009**
CD5	0,217	0,263	0,892	**0,013**
CD8A#	0,297	0,421	0,986	**0,002**
CDCP1#	0,664	0,445	0,763	**0,015**
CSF-1	**0,019**	**0,032**	0,205	**0,004**
CST5	0,082	0,288	0,840	**0,030**
CX3CL1	**0,026**	0,132	0,219	**0,006**
CXCL11	**0,108**	0,230	**0,027**	0,289
CXCL6	**0,012**	0,081	0,182	**0,005**
DNER	**0,029***	0,065	0,236	**0,011**
FGF-19#	0,115	0,116	0,759	**0,009**
Flt3L	**0,017**	0,087	0,312	**0,006**
HGF	**0,009**	0,148	0,824	**0,032**
IL-1 alpha#	0,849	0,007	0,097	0,532
IL-12B	0,132	0,519	0,761	**0,022**
IL-18R1#	0,274	0,360	0,750	**0,010**
IL-20RA	0,064	0,637	0,220	**0,032**
IL-10	0,072	**0,049**	0,265	0,087
IL-18	**0,003**	**0,031**	0,484	**0,012**
IL-33	**0,012**	**0,043**	0,743	**0,031**
IL-7	**0,029**	0,414	0,850	**0,036**
TGF-beta-1#	0,144	0,165	0,226	**0,011**
LIF	0,235	0,485	0,192	**0,030**
MCP-1#	0,060	0,303	0,365	**0,020**
MCP-2#	**0,043**	0,063	0,101	**0,014**
MCP-4	**0,001**	**0,005**	0,307	**0,002**
MMP-10	0,319	0,870	0,206	**0,014**
OPG	0,057	0,073	0,213	**0,003**
PD-L1	0,137	0,115	0,243	**0,009**
SCF	0,086	0,183	0,711	**0,046***
SIRT2	**0,002**	**0,014**	0,657	**0,002**
ST1A1#	0,772	0,987	**0,044**	0,173
STAMBP	**0,012**	**0,015**	0,733	**0,003**
TGF-alpha	0,293	0,088	0,701	**0,024**
TNF	0,233	0,057	0,595	**0,037**
TNFB	0,253	0,643	0,883	**0,009**
TNFSF14	**0,024**	0,124	0,087	0,064
TRAIL	**0,005**	**0,045**	0,290	**0,015**
TWEAK	**0,016**	0,092	0,919	0,071
uPA	0,074	0,144	0,965	**0,018**
VEGFA	0,169	0,079	0,547	**0,017**
4E-BP1	**0,018**	0,049	0,768	0,078
NOT Sign. Cytokines	*p-value* ***(> 0.05)***			
CD6	0,263	0,455	0,327	0,052
CXCL1#	0,357	0,110	0,635	0,058
CXCL10	0,104	0,214	0,118	0,224
CXCL5	0,074	0,064	0,170	0,109
CXCL9#	0,126	0,124	0,152	0,242
EN-RAGE	0,428	0,571	0,140	0,210
FGF-21#	0,091	0,659	0,090	0,407
IFN-gamma#	0,175	0,375	0,168	0,056
IL-10RB	0,086	0,271	0,649	0,093
IL-15RA	0,174	0,490	0,676	0,100
IL-17A	0,847	0,743	0,258	0,147
IL-17C#	0,451	0,357	0,559	0,072
IL6#	0,511	0,272	0,077	0,107
IL8	0,151	0,137	0,323	0,120
LIF-R	0,375	0,365	0,082	0,057
MMP-1#	0,942	0,962	0,633	0,063
OSM	0,080	0,137	0,132	0,108
TNFRSF9	0,220	0,600	0,939	0,075
TRANCE	0,246	0,550	0,738	0,121

 # cytokines where random factor addition significantly improved LOG2LME fit

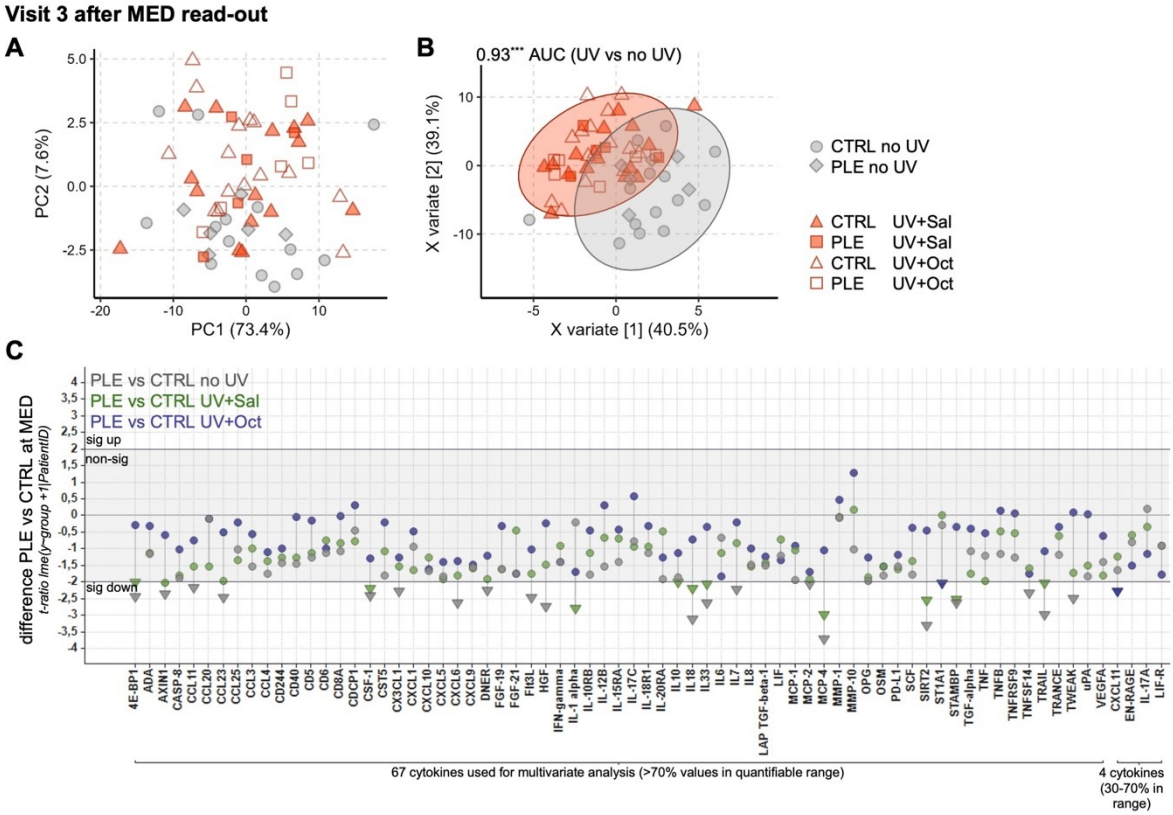

Figure 14 – Impaired cytokine production in PLE skin vs CTRL

A, PCA scores plot with each point representing the cytokine profile of the individual and proximity signifying similarity between individuals' 67 cytokine profile. The panel contains all samples from PLE (n = 6) and CTRL (n = 15), showing a weak difference along PC2 (y-axis) by exposure to UV. **B**, PLS-DA scores plot confirmed that UV exposure significantly changed the cytokine profiles by receiver operator curve (ROC) analysis with X variate 1-2 ($p < 0.05$). **C**, Dumbbell plot of all quantifiable 71 cytokines showing strength and significance (t ratios) of pairwise comparisons from LOG2LME analysis with all significant changes marked by triangles ($p < 0.05$). Most significant changes were observed in PLE vs CTRL in unexposed skin (black) with cytokine levels being lower in PLE. After UV exposure cytokine levels in PLE became more similar to CTRL in saline (green) and nearly normalized after disinfection becoming non-significant (brown).

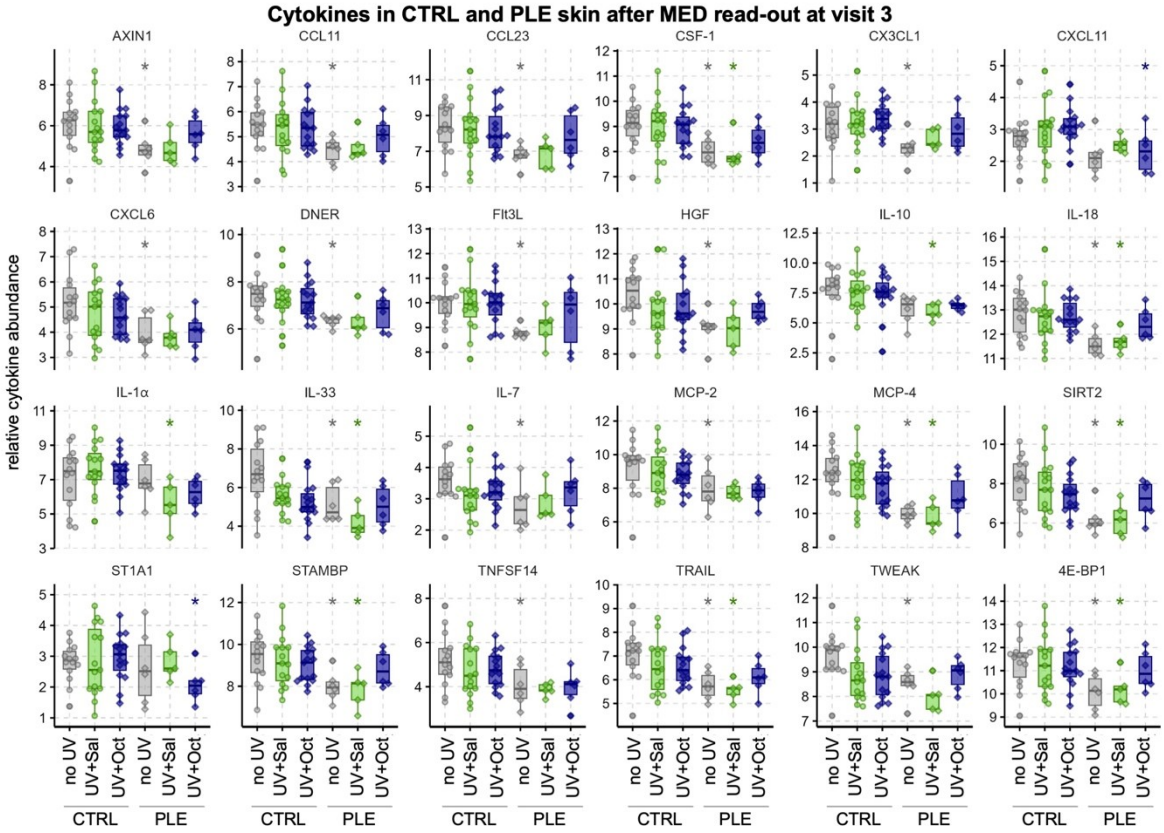

Figure 15 – Cytokine levels in PLE skin vs CTRL at MED level

Box plots of 24 cytokines with any significance in one of the three comparisons of interest: PLE vs CTRL at the same field in grey – unexposed, green – UV+Sal, brown – UV+Oct. All significances from LOG2LME are marked by an * ($p < 0.05$) in the same colour. The middle line in each box marks the median, box edges mark the first and third quartile, the whiskers show the 1.5-fold interquartile data range and all measurements are shown as single points.

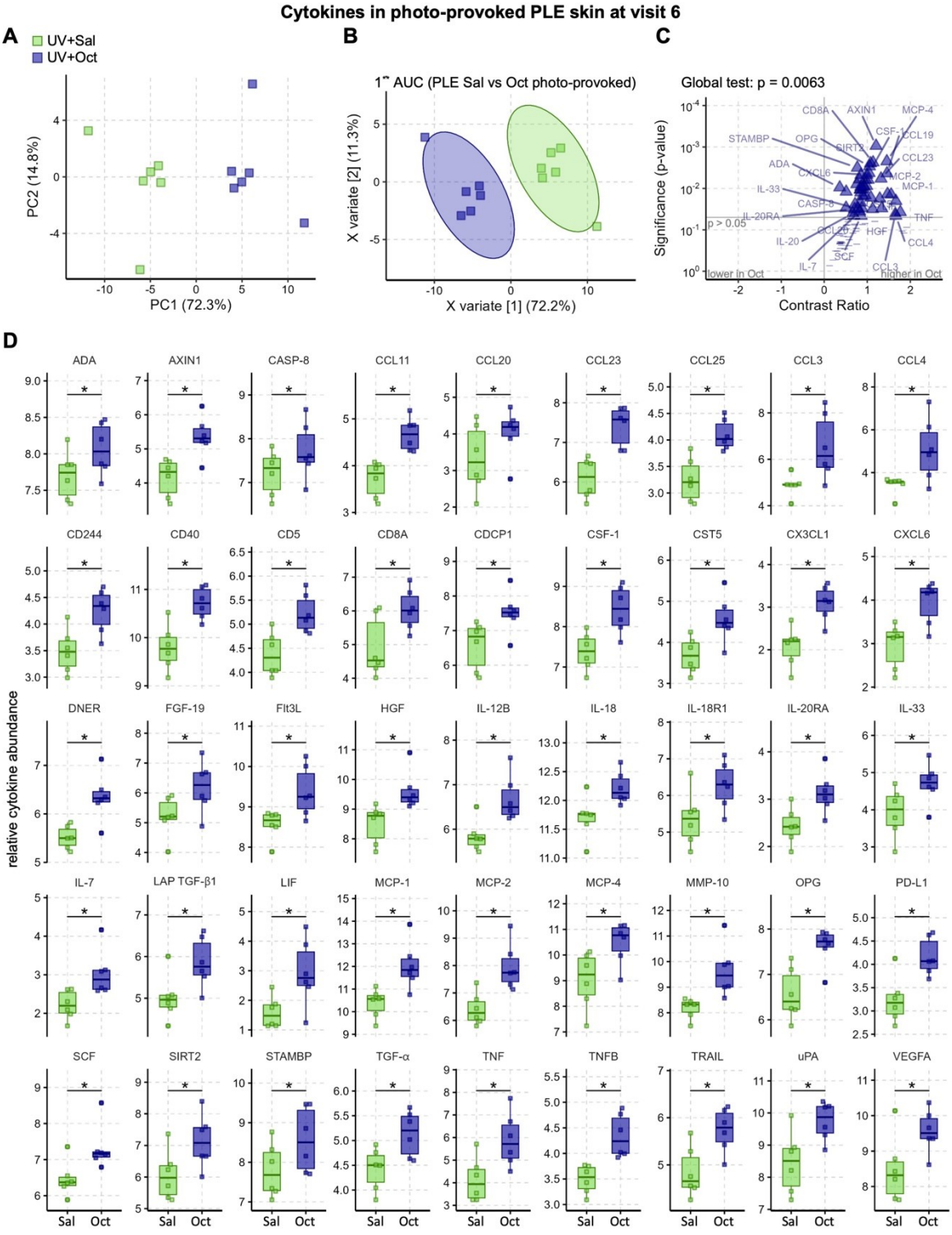

Figure 16 – Increased cytokine production photoprovoked PLE skin

A, PCA scores plot with each point representing the 67 cytokine profile from PLE patients (n = 6) saline or disinfected skin blisters after photoprovocation (visit 6). **B**, PLS-DA scores plot confirmed that disinfection significantly changed the cytokine profiles by receiver operator curve (ROC) analysis with X variate 1-2 ($p < 0.05$). **C**, Volcano plot of LOG2LME pairwise comparison of disinfected to saline treaded PLE skin blister cytokines showing a strong and significant increase in 45 cytokines ($p < 0.05$). Horizontal line marks $p = 0.05$ and

vertical line marks zero change. The global test result is shown, performed according to Goeman et al. **D**, Box plots of the 45 significantly increased cytokines (* $p < 0.05$). The middle line in each box marks the median, box edges mark the first and third quartile, the whiskers show the 1.5-fold interquartile data range and all measurements are shown as single points.

3.6 Microbiome-related modulation of inflammatory pathways in PLE

To identify the most relevant signaling pathways in photoprovoked PLE skin, comparing saline treatment to disinfection, the corresponding UniProt IDs of the 45 significantly altered cytokines from blister fluid analysis (Figure 17, Table 4) were subjected to STRING database. STRING is a widely used bioinformatics tool for analyzing protein-protein interactions, providing functionality for enrichment analysis and subsequent visualization (55).

First, a network of both physical and functional associated protein-protein interactions was generated (Figure 17). This approach allowed to identify s signaling pathways of protein-protein-interactions.

The top signaling pathways identified through the enrichment analysis included positive regulation of chronic inflammatory response to antigenic stimulus, T-helper 1 cell cytokine production, positive regulation of NK T cell proliferation, positive regulation of humoral immune response mediated by circulating immunoglobulin, eosinophil chemotaxis, regulation of natural killer cell chemotaxis, Interleukin-18-mediated signaling, positive regulation of macrophage differentiation, death-inducing signaling complex assembly, macrophage chemotaxis, and lymphocyte chemotaxis (Table 4). These results represent the top 11 pathways based on their significance and relevance to PLE.

It is important to note that the enrichment analysis results were corrected for pathways that may belong to other organ systems, ensuring that the identified pathways are specifically relevant to PLE skin.

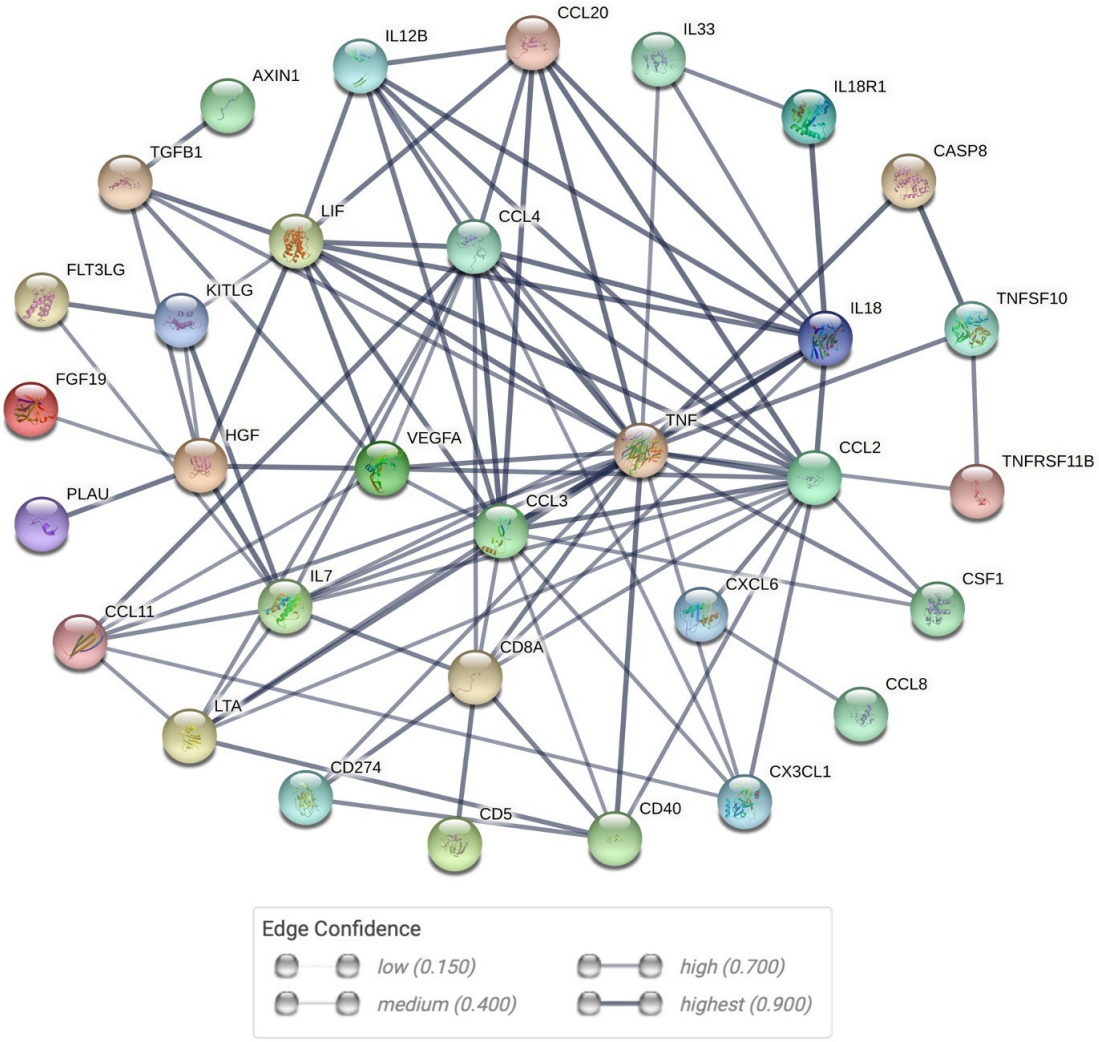

Figure 17 – Protein-protein interaction network analysis in PLE

STRING-database-analysis of significantly changed blister fluid cytokines of disinfected UV-exposed skin compared to saline-treated UV-exposed skin after the 4th photoprovocation of PLE patients (visit 6). Line thickness indicates the strength of data support. The edges indicate both functional and physical protein associations. Pre-adjustments were set to only show protein-protein-interactions with high edge confidence.

Table 4 – Enriched signaling pathways in photoprovoked PLE skin

signalling pathway	*protein-protein interaction (saline vs. disinfection)*	*strength*	*false discovery rate*
Positive regulation of chronic inflammatory response to antigenic stimulus	TNF,LTA	2.64	0.0012
T-helper 1 cell cytokine production	IL12B,IL18	2.34	0.0026
Positive regulation of nk t cell proliferation	IL12B,IL18	2.34	0.0026
Positive regulation of humoral immune response mediated by circulating immunoglobulin	TNF,LTA	2.24	0.0035
Eosinophil chemotaxis	CX3CL1,CCL2,CCL13,CCL11, CCL8,CCL3,CCL23	2.2	$1.99e^{-11}$
Regulation of natural killer cell chemotaxis	CCL2,CCL3,CCL4	2.16	0.0044
interleukin-18-mediated signaling pathway	IL18,IL18R1	2.09	0.0053
Positive regulation of macrophage differentiation	TGFB1,LIF,CSF1,CASP8	2.06	$5.76e^{-06}$
Death-inducing signaling complex assembly	CASP8,TNF	2.04	0.0063
Macrophage chemotaxis	CX3CL1,CCL2,CCL3	1.97	0.00034
Lymphocyte chemotaxis	CX3CL1,CCL2,CCL13,CCL11, CCL20,CCL25,CCL8,CCL3, CCL23,CCL4	1.94	$2.93e^{-14}$

3.7 Histopathological comparison of treatment effects in PLE skin

The aim of blister roof sample collection was performed to provide another layer of information for potential further analysis. These analyses including immunohistochemistry staining's or gene expression analysis could provide insights into the cellular and molecular changes occurring in the epidermis.

Skin biopsies were obtained from three patients with polymorphic light eruption (PLE) to examine the histopathological changes associated with different treatment approaches. Specifically, biopsies were taken from disinfected, photoprovoked PLE skin and saline-treated, photoprovoked PLE skin. Upon histological evaluation, the density of infiltrate was assessed as a key parameter to compare the treatment effects. In two out of the three patients, the findings aligned with the hypothesis, revealing a stronger histological manifestation of PLE in terms of increased infiltrate density in the disinfected, photoprovoked skin samples. In one patient, a contrasting trend was observed (Figure 19, Table 5).

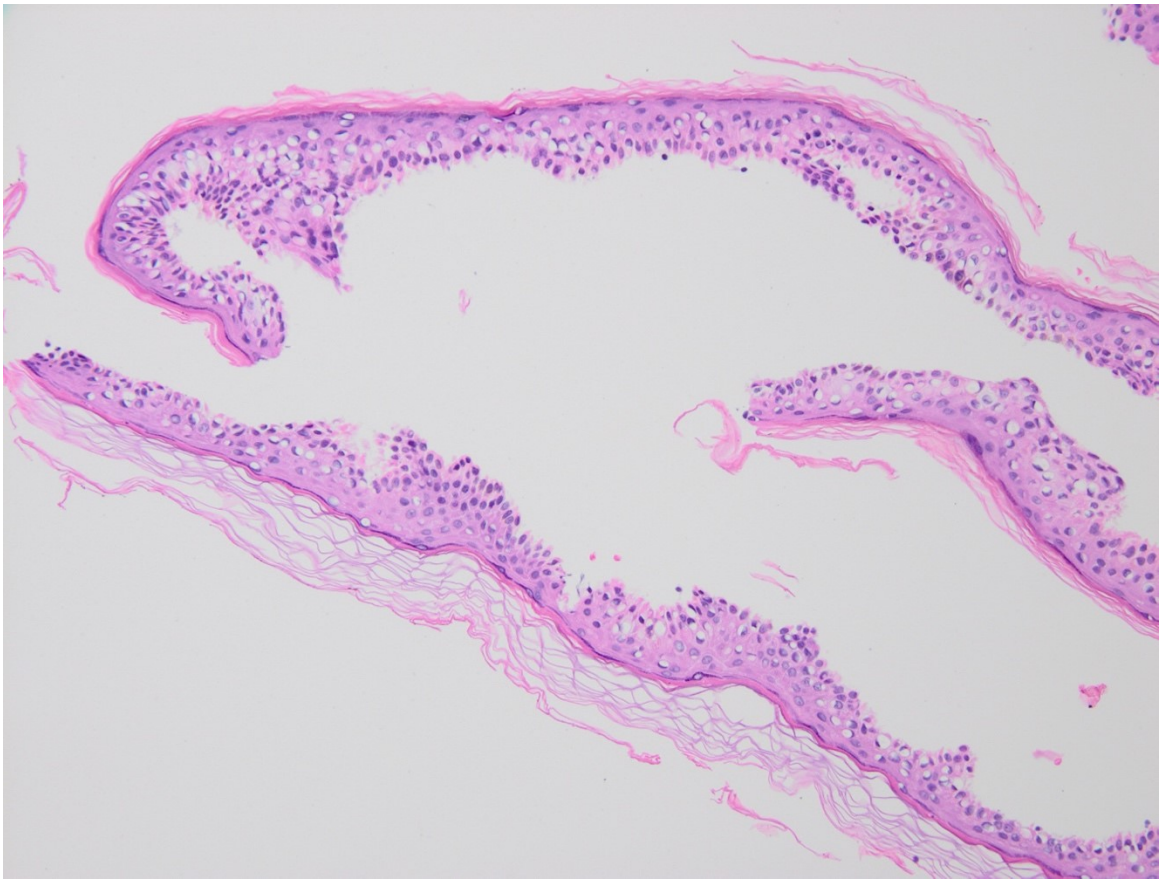

Figure 18 – Histological image of a H/E-stained blister roof

Table 5 – Histopathological evaluation of photoprovoked PLE skin

PLE ID	Treatment	Histopathological evaluation	Densitiy of infiltrate
P1	NaCl	PLE with pervivascular lymphocytic infiltrates	NaCl > Octeniderm®
P1	Octeniderm®	less specific and less infiltrate	
P4	NaCl	sparse infiltrate	Octeniderm® > NaCl
P4	Octeniderm®	PLE, with pervivascular lymphocytic infiltrates	
P10	NaCl	PLE, massive infiltrate, Neutrophils	NaCl > Octeniderm®
P10	Octeniderm®	PLE	

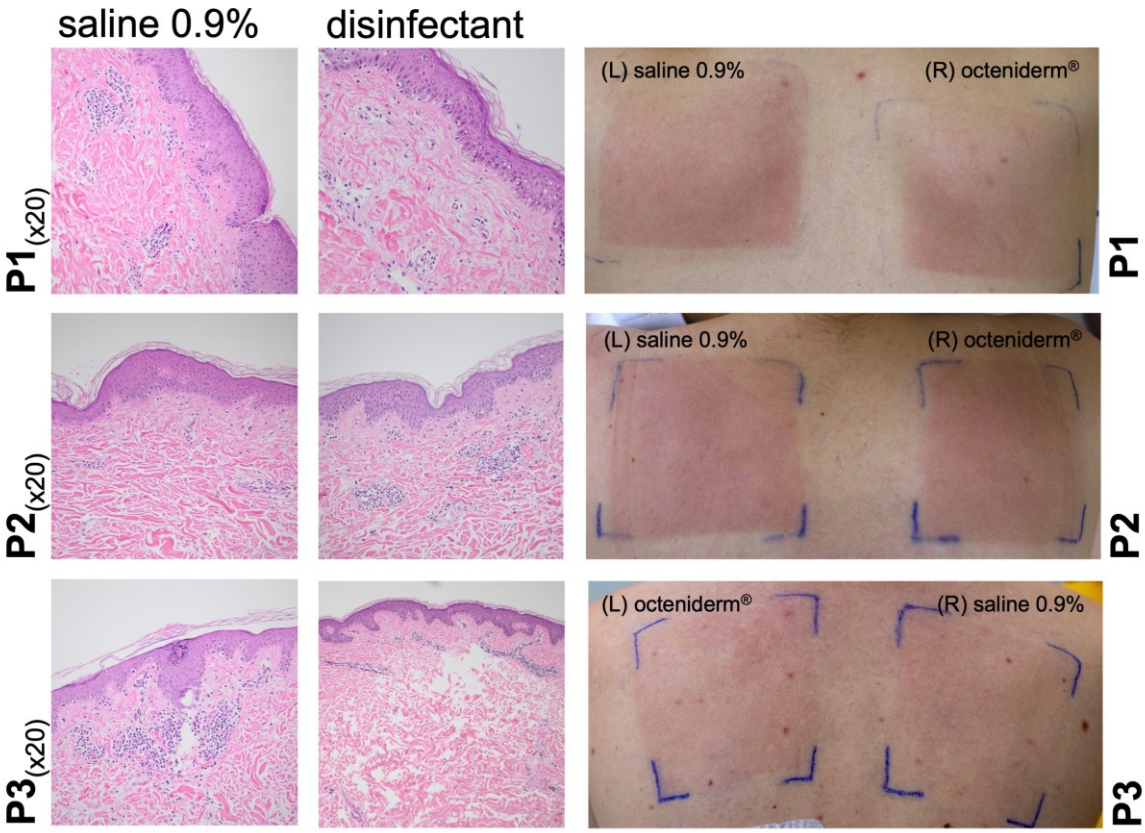

Figure 19 – Histopathological comparison of photoprovoked PLE skin

4. Discussion

4.1 Summary of results

In light of this study's findings, it appears that patients with PLE exhibit a lower overall cytokine production compared to healthy subjects, irrespective of UV exposure (Figure 15). Surprisingly, none of the cytokines with any significance in expression were differentially upregulated (Figure 14C, Figure 15), which is consistent with a previous study in PLE (56). The fact that this pattern is most pronounced in unexposed skin may suggest that PLE patients exhibit a state of 'immune hypo-responsiveness' at baseline, as these lower expressed cytokines are crucial for a wide range of immune functions including inflammation, immune cell recruitment, cell growth, and differentiation. For instance, lower levels of chemokines like CCL11, CCL23, CX3CL1, CXCL6, MCP-2, and MCP-4 could impair immune cell migration and recruitment to sites of inflammation, compromising the skin's ability to respond adequately to UV-induced damage. Additionally, reduced expression of interleukins such as IL-7, IL-18, IL-33, may lead to a dysregulated inflammatory response, increasing susceptibility of exacerbating UV-induced skin reactions. Notably, the lower expression of cytokines such as TWEAK and TRAIL, both known to induce apoptosis, add implications

towards observations Lembo et. al., who reported an accumulation of apoptotic cells in PLE patients exposed to UVB or UVA1 (57). This indication towards a potential dysregulation or attenuation of apoptotic processes in PLE may contributing to the abnormal response to UVR. Furthermore, growth factors like Flt3L and HGF could impact cell growth and tissue regeneration, possibly affecting the skin's resilience against UV damage and might affect barrier function. The decrease in proteins like AXIN1, DNER, SIRT2, STAMPB, and 4EBP1, which are involved in cell differentiation, stress responses, and protein synthesis, may also contribute to an overall perturbation of skin cell behavior and function in PLE.

Upon UV exposure in saline-treated MED skin, the cytokine dysregulation is less pronounced, possibly as a result of UV-induced modulation of cytokine expression (Figure 15). Nevertheless, the dysregulation appears to persist to some extent, as indicated by the continued underexpression of 9 out of 11 cytokines (CSF-1, IL-18, IL-33, MCP-4, SIRT2, STAMPB, TRAIL, 4EBP1) that are similarly underexpressed in unexposed, untreated skin when comparing PLE vs. CTRL (Figure 15). This observation underscores the persistence of an underlying cytokine imbalance in PLE, which persists even under conditions of a single UV exposure at MED.

Interestingly, disinfection and UV-exposure at MED-level nearly fully restored cytokine imbalance of PLE vs. CTRL, except for 2 underexpressed cytokines (ST1A1, CXCL11) that differ from the cytokine profiles of both unexposed skin, and saline-treated, UV-exposed skin (Figure 15). This could potentially be linked to the involvement of skin microbiota in the impairment of UV-induced immunosuppression in PLE (7,58).

After multiple, mild UV exposures in PLE patients, this trend of cytokine modulation towards a normalized cytokine pattern in terms of cytokine values, was even more significant (Figure 16D). This observation further underlines a potential link between the skin microbiome and its modulatory capacity in PLE immune response to UVR.

Histopathological evaluation of photoprovoked skin suggests that disinfection might have an impact on the inflammatory response in PLE, based on a tendency to lower density of infiltrate within a low number of samples (Figure 19, Table 5).

However, despite the low PLE Score observed in our patient cohort, which did not reveal any significant clinical differences between disinfection or not, a clear impairment at the cytokine level could still be observed, as described above (Figure 7). It is important to note that cytokine expression was measured during an early time frame after UV exposure. Given that PLE is described as a delayed-type hypersensitivity reaction to UVR, the timepoint of

cytokine determination may reflect a cytokine pattern prior to PLE exacerbation in patients that are inherently mildly affected by the disease. Further explanations for this outcome might include a slightly lower intensity in the UVA spectrum of the phototesting device used, as well as the choice of body area for testing, which was the back of the subjects (Figure 2). This body area is not known to be a predilection site where PLE usually develops, such as the V-area or the upper arms (3). Hence, the observed differences in the severity of disease manifestation could be due to various factors. For instance, differences in microstructural skin properties, abundance of certain immune cells and a differential microbial landscape as compared to more typical PLE-affected areas. This assumption highlights the importance of considering the potential impact of the skin microbiome's spatial variability on disease presentation and immune response at different body sites in future studies.

Moreover, the observed low read counts in most of the samples of the microbiome analysis highlight the need for further optimization and enhancement of the sequencing process to achieve an adequate sequencing depth (Figure 9). Hence, the observed microbial composition does not allow an interpretation and should be considered as a test of procedure.

Overall cis-UCA levels in control subjects were higher compared to PLE patients, irrespective of treatment (Figure 8). This implies that the overall synthesis or accumulation of cis-UCA appears to be diminished in PLE patients. While these trends provide important insights into the possible role of cis-UCA in PLE pathophysiology, these findings should be considered preliminary, due to the limited sample size and the sampling method, which is recommended differently in a recent review (59).

4.2 Potential bias

The design and execution of this pilot study were not without potential sources of bias, each potentially affecting the interpretation and reproducibility of the results.

Firstly, the study was conducted in spring, a period where natural photo hardening can already start, especially in warm and sunny periods as of spring 2021. This seasonal effect might have influenced the participant's response to UV radiation, potentially confounding the results by reducing UV sensitivity, particularly in PLE patients (29,59).

The recruitment process also posed a potential source of bias. Of the participants in the PLE group, three individuals were recruited from the registry of photodermatoses of the Unit for Photodermatology, Graz, with a definitive diagnosis of PLE. The remaining 3 individuals from PLE group, were included based on their patient history and photographic evidence

suggestive of PLE. However, a definitive diagnosis of PLE of those participants, who were not recruited from the photodermatoses registry, could only be confirmed in one of these patients, who consented to a skin biopsy. In the remaining two participants, despite anamnesis highly suggestive of PLE, the lack of definitive phototest or histopathological confirmation poses a potential misclassification bias.

Potential bias was also present in our tape strip method for cis-UCA collection. The first three tape strips were discarded as per the manufacturer's recommendation, possibly discarding a substantial amount of cis-UCA in the process. A comprehensive review of the tape stripping method, published after the completion of the clinical part of our pilot study, recommended instead using the first 4 tape strips (59). Our current results may therefore represent only a fraction of the cis-UCA concentration levels that might have been detected with the most recently recommended collection method.

A potential limitation that warrants consideration lays within the cytokine immune assay that has been used. Despite an initial pilot study conducted by Olink® to check the quality and significance of their proximity extension assay, we did not validate the proteomic data with any other type of immune assay. This could potentially lead to a lack of comparability and reproducibility in the assay results.

Finally, the results of the pathway enrichment analysis showing a modified list of the top regulated pathways should be interpreted with caution and are best used as a form of orientation to provide insights into the regulatory pathways involved in the inflammatory response after photoprovocation in PLE patients. Typically, pathway enrichment analysis is conducted by using a reference set that is relevant to the biological question at hand (60). This could be the entire genome, or all the genes assessed in the study, or a disease-specific reference set. In this study, however, the Homo sapiens genome was used as the reference set for the analysis, which may not be the most appropriate choice given the context of the study. Moreover, the pathways associated with other organs were excluded from the analysis. While this decision was scientifically sound, it introduced a major bias by removing certain relevant biological processes from the analysis.

4.3 Limitations and complications

This pilot study was conducted under several limitations and encountered various complications, each influencing the comprehensive acquisition of data and subsequent interpretation of results.

First and foremost, the recruitment process was significantly affected by the Covid-19 pandemic in terms of willingness to engage in the study. The health concerns associated with the pandemic were particularly notable in the case of potential PLE patients. Consequently, this significantly impacted the statistical power of the study results due to the reduced sample size.

The issue of participant consent also presented a challenge in the collection of skin biopsy samples. With only three PLE patients consenting to the procedure, the sample size was too small to allow for statistically robust intra-individual comparisons of photoprovoked disinfected and saline-treated skin (visit 6).

Another significant obstacle was encountered when an unforseen sensor defect in the instrument used to measure trans-epidermal water loss (TEWL) was identified close to the study's commencement. Due to the already scheduled visits of study participants, it was not possible to repair or replace the TEWL probe in a timely manner. New probe heads and instruments have been acquired in the meantime for future studies.

Additionally, the initial plan to conduct single-cell-RNA sequencing for transcriptomic analysis had to be shelved due to too low T-cell counts in the blister fluid. This suggested that the volume of fluid obtainable from the blisters was insufficient for this type of analysis. Given the constraints on the test field size, which precluded the formation of larger or additional blisters, the decision was made to step back from transcriptomic analysis.

The skin swabs were insufficient to obtain sufficient biomass, which directly translated in the low number of reads in 16S sequencing. Consequently, the analysis captured only a fraction of the actual microbial landscape. A more intense and comprehensive application of the swabs might have overcome this issue, which is critical for obtaining adequate biomass for 16S sequencing.

4.4 Current state and outlook

In the landscape of polymorphic light eruption (PLE) treatment, recent advances have explored a broad spectrum of therapeutic strategies. One such innovative therapeutic approach is the use of the α-melanocyte stimulating hormone analogue, Afamelanotide, which induces skin pigmentation and presents photoprotective properties and is used for treatment in erythropoietic protoporphyria (61,62). Furthermore, the role of the cytokine IL-31 in the pathogenesis of PLE-associated pruritus is receiving increasing attention and has been recognized as a potential therapeutic target (63). Anti-IL-31 monoclonal antibody (Nemolizumab) is one such promising treatment, that has been successfully used to treat

moderate to severe itch in patients with atopic dermatitis and prurigo nodularis, suggesting potential effectiveness in PLE (64,65). While these novel therapies represent significant advancements, their economic feasibility remains a crucial concern, considering the high prevalence of PLE and its limitation to severe cases. Those critical aspects are prompting research to revisit and refine traditional preventative and therapeutic approaches.

For instance, photoprotective measures, such as avoiding intense sunlight, using sun-protective clothing, and applying broad-spectrum sunscreens, remain fundamental strategies for PLE management (13). Research in photoprotection suggests that sunscreens containing DNA repair enzymes like photolyase and T4 endonucleases may further enhance these effects by promoting DNA repair and eliminating UV-induced DNA photoproducts (38).

Additionally, probiotic treatment holds promise as a potential therapeutic approach for skin diseases, including polymorphic light eruption (PLE) (66). Emerging evidence suggests that probiotics can modulate the immune response and restore microbial homeostasis, thereby influencing the pathogenesis of skin disorders (67). By promoting a healthy skin microbiome and enhancing the skin's barrier function, probiotics may help alleviate the symptoms of PLE and reduce the frequency and severity of flare-ups (68). However, further research is needed to elucidate the specific mechanisms by which probiotics exert their beneficial effects and to determine the optimal strains, dosages, and treatment durations for PLE patients.

Similarly, oral vitamin D supplementation, which can correct the vitamin D insufficiency often observed in PLE patients, may not only restore immune balance but also provide photoprotective effects (69). Topically applied calcipotriol, a vitamin D3 analogue, has been shown to decrease the number and function of epidermal Langerhans cells (LCs), thus potentially preventing PLE lesions (37).

Furthermore, phototherapy remains a viable preventative option for severe PLE cases (14). Clinical photohardening, or the controlled gradual exposure to UV radiation, promotes photoadaptation without provoking an eruption and mitigates some of the immunological abnormalities observed in PLE (70).

Given the evolving therapeutical options in PLE, it is crucial to note that elucidating the underlying mechanisms of PLE remains a central focus of ongoing research. It is well established that sunlight triggers a series of immunological events that ultimately result in PLE eruptions (13). However, the precise mechanisms remain unclear. Future research in this area utilizing powerful novel analysis approaches such as spatial transcriptomics, may further unravel the role of various immune cells in specific skin areas(71). Of special interest

are Langerhans cells and specific T cell subtypes, the cytokines they produce in the initiation and progression of PLE, as well as the intricate relationship between skin microorganisms and how it influences the pathogenesis of PLE. Moreover, it would be valuable to investigate the temporal dynamics of the skin microbiome and its influence on cytokine regulation by examining the changes in the skin microbiome and cytokine profiles over time. Those insights would potentially pave the way to provide novel therapeutic approaches for the development of targeted interventions to modulate the skin microbiome.

5. Conclusion

This pilot study provided a minimal-invasive concept for *in vivo* analysis of immune responses in dependence of skin microbiome and UVR in PLE patients compared to healthy subjects. Despite the fact that disinfection of PLE skin had no clinically strong effects upon exposure to UVR, the study's findings reveal additional implications in the dysregulated immune response underlying PLE, indicating an involvement of skin microbiome. Future studies with larger cohorts and refined sampling procedures are needed to confirm and expand upon these findings. A more comprehensive exploration of the specific immunological pattern in different phases of PLE manifestation and a deeper understanding of the crosstalk with skin microbiota remains to be observed.

Bibliography

1. Bernard JJ, Gallo RL, Krutmann J. Photoimmunology: how ultraviolet radiation affects the immune system. *Nature reviews. Immunology*. 2019;19(11): 688–701. https://doi.org/10.1038/S41577-019-0185-9.
2. Narayanan DL, Saladi RN, Fox JL. Ultraviolet radiation and skin cancer. *International journal of dermatology*. 2010;49(9): 978–986. https://doi.org/10.1111/J.1365-4632.2010.04474.X.
3. Gruber-Wackernagel A, Byrne SN, Wolf P. Polymorphous light eruption: clinic aspects and pathogenesis. *Dermatologic clinics*. 2014;32(3): 315–334. https://doi.org/10.1016/J.DET.2014.03.012.
4. Lembo S, Fallon J, O'Kelly P, Murphy GM. Polymorphic light eruption and skin cancer prevalence: is one protective against the other? *The British journal of dermatology*. 2008;159(6): 1342–1347. https://doi.org/10.1111/J.1365-2133.2008.08734.X.
5. Ali N, Rosenblum MD. Regulatory T cells in skin. *Immunology*. 2017;152(3): 372–381. https://doi.org/10.1111/IMM.12791.
6. Burns EM, Ahmed H, Isedeh PN, Kohli I, Van Der Pol W, Shaheen A, et al. Ultraviolet radiation, both UVA and UVB, influences the composition of the skin microbiome. *Experimental dermatology*. 2019;28(2): 136–141. https://doi.org/10.1111/EXD.13854.
7. Patra VK, Byrne SN, Wolf P. The skin microbiome: Is it affected by UV-induced immune suppression? *Frontiers in Microbiology*. 2016;7(AUG). https://doi.org/10.3389/fmicb.2016.01235.
8. Sinha S, Lin G, Ferenczi K. The skin microbiome and the gut-skin axis. *Clinics in Dermatology*. 2021;39(5): 829–839. https://doi.org/10.1016/j.clindermatol.2021.08.021.
9. Oh J, Freeman AF, Park M, Sokolic R, Candotti F, Holland SM, et al. The altered landscape of the human skin microbiome in patients with primary immunodeficiencies. *Genome research*. 2013;23(12): 2103–2114. https://doi.org/10.1101/GR.159467.113.
10. Patra VK, Laoubi L, Nicolas JF, Vocanson M, Wolf P. A perspective on the interplay of ultraviolet-radiation, skin microbiome and skin resident memory TCRαβ+ cells. *Frontiers in Medicine*. 2018;5(MAY): 1–9. https://doi.org/10.3389/fmed.2018.00166.
11. Rhodes LE. Polymorphic Light Eruption Occurs in 18 % of Europeans and Does Not Show Higher Prevalence with Increasing Latitude : Multicenter Survey of 6 , 895 Individuals Residing from the Mediterranean to Scandinavia. *Journal of Investigative Dermatology*. 2010;130(2003): 626–628. https://doi.org/10.1038/jid.2009.250.
12. Wolf P, Byrne SN, Gruber-wackernagel A. New insights into the mechanisms of polymorphic light eruption: resistance to ultraviolet radiation-induced immune suppression as an aetiological factor. *Experimental Dermatology*. 2009;18(4): 350–356. https://doi.org/10.1111/J.1600-0625.2009.00859.X.
13. Kadurina M, Kazandjieva J, Bocheva G. Immunopathogenesis and management of polymorphic light eruption. *Dermatologic therapy*. 2021;34(6). https://doi.org/10.1111/DTH.15167.
14. Yu Z, Wolf P. How It Works: The Immunology Underlying Phototherapy. *Dermatologic Clinics*. 2020;38(1): 37–53. https://doi.org/10.1016/j.det.2019.08.004.

15. Ling TC, Richards HL, Janssens AS, Anastassopoulou L, Antoniou C, Aubin F, et al. Seasonal and latitudinal impact of polymorphic light eruption on quality of life. *The Journal of investigative dermatology*. 2006;126(7): 1648–1651. https://doi.org/10.1038/SJ.JID.5700306.
16. Rutter KJ, Ashraf I, Cordingley L, Rhodes LE. Quality of life and psychological impact in the photodermatoses: a systematic review. *The British journal of dermatology*. 2020;182(5): 1092–1102. https://doi.org/10.1111/BJD.18326.
17. Millard TP, Bataille V, Snieder H, Spector TD, McGregor JM. The heritability of polymorphic light eruption. *The Journal of investigative dermatology*. 2000;115(3): 467–470. https://doi.org/10.1046/J.1523-1747.2000.00079.X.
18. McGregor JM, Grabczynska S, Vaughan R, Hawk JLM, Lewis CM. Genetic modeling of abnormal photosensitivity in families with polymorphic light eruption and actinic prurigo. *The Journal of investigative dermatology*. 2000;115(3): 471–476. https://doi.org/10.1046/J.1523-1747.2000.00080.X.
19. Kurz B, Arndt S, Unger P, Ivanova I, Berneburg M, Hellerbrand C, et al. Association of polymorphous light eruption with NOD-2 and TLR-5 gene polymorphisms. *Journal of the European Academy of Dermatology and Venereology : JEADV*. 2022;36(11): 2172–2180. https://doi.org/10.1111/JDV.18364.
20. Goethel A, Turpin W, Rouquier S, Zanello G, Robertson SJ, Streutker CJ, et al. Nod2 influences microbial resilience and susceptibility to colitis following antibiotic exposure. *Mucosal immunology*. 2019;12(3): 720–732. https://doi.org/10.1038/S41385-018-0128-Y.
21. Kawai T, Akira S. TLR signaling. *Seminars in immunology*. 2007;19(1): 24–32. https://doi.org/10.1016/J.SMIM.2006.12.004.
22. Holler E, Rogler G, Brenmoehl J, Hahn J, Greinix H, Dickinson AM, et al. The role of genetic variants of NOD2/CARD15, a receptor of the innate immune system, in GvHD and complications following related and unrelated donor haematopoietic stem cell transplantation. *International journal of immunogenetics*. 2008;35(4–5): 381–384. https://doi.org/10.1111/J.1744-313X.2008.00795.X.
23. Lembo S, Raimondo A. Polymorphic Light Eruption: What's New in Pathogenesis and Management. *Frontiers in medicine*. 2018;5(SEP). https://doi.org/10.3389/FMED.2018.00252.
24. Palmer RA, Friedmann PS. Ultraviolet Radiation Causes Less Immunosuppression in Patients with Polymorphic Light Eruption Than in Controls. *Journal of Investigative Dermatology*. 2004;122(2): 291–294. https://doi.org/10.1046/J.0022-202X.2004.22213.X.
25. Schornagel IJ, Sigurdsson V, Nijhuis EHJ, Bruijnzeel-Koomen CAFM, Knol EF. Decreased neutrophil skin infiltration after UVB exposure in patients with polymorphous light eruption. *Journal of Investigative Dermatology*. 2004;123(1): 202–206. https://doi.org/10.1111/j.0022-202X.2004.22734.x.
26. Wolf P, Gruber-Wackernagel A, Bambach I, Schmidbauer U, Mayer G, Absenger M, et al. Photohardening of polymorphic light eruption patients decreases baseline epidermal Langerhans cell density while increasing mast cell numbers in the papillary dermis. *Experimental Dermatology*. 2014;23(6): 428–430. https://doi.org/10.1111/exd.12427.
27. Schweintzger NA, Gruber-Wackernagel A, Shirsath N, Quehenberger F, Obermayer-Pietsch B, Wolf P. Influence of the season on vitamin D levels and regulatory T cells in patients with polymorphic light eruption. *Photochemical & photobiological sciences : Official journal of the European Photochemistry Association and the*

European Society for Photobiology. 2016;15(3): 440–446. https://doi.org/10.1039/C5PP00398A.
28. Schweintzger N, Gruber-Wackernagel A, Reginato E, Bambach I, Quehenberger F, Byrne SN, et al. Levels and function of regulatory T cells in patients with polymorphic light eruption: Relation to photohardening. *British Journal of Dermatology*. 2015;173(2): 519–526. https://doi.org/10.1111/bjd.13930.
29. Patra VK, Strobl J, Atzmüller D, Reininger B, Kleissl L, Gruber-Wackernagel A, et al. Accumulation of Cytotoxic Skin Resident Memory T Cells and Increased Expression of IL-15 in Lesional Skin of Polymorphic Light Eruption. *Frontiers in medicine*. 2022;9. https://doi.org/10.3389/FMED.2022.908047.
30. Patra VK, Wolf P. *Microbial elements as the initial triggers in the pathogenesis of polymorphic light eruption?*. Experimental Dermatology. 2016. p. 999–1001. https://doi.org/10.1111/exd.13162.
31. Patra VK, Wolf P. *Microbial elements as the initial triggers in the pathogenesis of polymorphic light eruption?*. Experimental Dermatology. 2016. p. 999–1001. https://doi.org/10.1111/exd.13162.
32. Harder J, Gläser R, Schröder JM. Human antimicrobial proteins effectors of innate immunity. *Journal of endotoxin research*. 2007;13(6): 317–338. https://doi.org/10.1177/0968051907088275.
33. Gläser R, Harder J, Lange H, Bartels J, Christophers E, Schröder JM. Antimicrobial psoriasin (S100A7) protects human skin from Escherichia coli infection. *Nature immunology*. 2005;6(1): 57–64. https://doi.org/10.1038/NI1142.
34. Guaní-Guerra E, Santos-Mendoza T, Lugo-Reyes SO, Terán LM. Antimicrobial peptides: general overview and clinical implications in human health and disease. *Clinical immunology (Orlando, Fla.)*. 2010;135(1): 1–11. https://doi.org/10.1016/J.CLIM.2009.12.004.
35. Patra VK, Mayer G, Gruber-Wackernagel A, Horn M, Lembo S, Wolf P. Unique profile of antimicrobial peptide expression in polymorphic light eruption lesions compared to healthy skin, atopic dermatitis, and psoriasis. *Photodermatology Photoimmunology and Photomedicine*. 2018;34(2): 137–144. https://doi.org/10.1111/phpp.12355.
36. Patra VK, Wagner K, Arulampalam V, Wolf P. Skin Microbiome Modulates the Effect of Ultraviolet Radiation on Cellular Response and Immune Function. *iScience*. 2019;15: 211–222. https://doi.org/10.1016/j.isci.2019.04.026.
37. Gruber-Wackernagel A, Bambach I, Legat FJ, Hofer A, Byrne SN, Quehenberger F, et al. Randomized double-blinded placebo-controlled intra-individual trial on topical treatment with a 1,25-dihydroxyvitamin D 3 analogue in polymorphic light eruption. *British Journal of Dermatology*. 2011;165(1): 152–163. https://doi.org/10.1111/j.1365-2133.2011.10333.x.
38. Hofer A, Legat FJ, Gruber-Wackernagel A, Quehenberger F, Wolf P. Topical liposomal DNA-repair enzymes in polymorphic light eruption. *Photochemical and Photobiological Sciences*. 2011;10(7): 1118–1128. https://doi.org/10.1039/c1pp05009e.
39. Dapic I, Jakasa I, Yau NLH, Kezic S, Kammeyer A. Evaluation of an HPLC Method for the Determination of Natural Moisturizing Factors in the Human Stratum Corneum. *Analytical Letters*. 2013;46(14): 2133–2144. https://doi.org/10.1080/00032719.2013.789881.
40. Odendaal ML, Groot JA, Hasrat R, Chu MLJN, Franz E, Bogaert D, et al. Higher off-target amplicon detection rate in MiSeq v3 compared to v2 reagent kits in the

context of 16S-rRNA-sequencing. *Scientific Reports*. 2022;12(1): 16489. https://doi.org/10.1038/S41598-022-20573-1.
41. Strassner JP, Rashighi M, Ahmed Refat M, Richmond JM, Harris JE. Suction blistering the lesional skin of vitiligo patients reveals useful biomarkers of disease activity. *Journal of the American Academy of Dermatology*. 2017;76(5): 847-855.e5. https://doi.org/10.1016/j.jaad.2016.12.021.
42. Hall M, Beiko RG. 16S rRNA Gene Analysis with QIIME2. *Methods in molecular biology (Clifton, N.J.)*. 2018;1849: 113–129. https://doi.org/10.1007/978-1-4939-8728-3_8.
43. *R: The R Project for Statistical Computing*. https://www.r-project.org/ [Accessed 30th May 2023].
44. McMurdie PJ, Holmes S. phyloseq: an R package for reproducible interactive analysis and graphics of microbiome census data. *PloS one*. 2013;8(4). https://doi.org/10.1371/JOURNAL.PONE.0061217.
45. Rohart F, Gautier B, Singh A, Lê Cao KA. mixOmics: An R package for 'omics feature selection and multiple data integration. *PLoS computational biology*. 2017;13(11). https://doi.org/10.1371/JOURNAL.PCBI.1005752.
46. Muaidi QI, Ahsan M. Measurement of visceral fat, abdominal circumference and waist-hip ratio to predict health risk in males and females. *Pakistan Journal of Biological Sciences*. 2019;22(4): 168–173. https://doi.org/10.3923/PJBS.2019.168.173.
47. Jo JH, Kennedy EA, Kong HH. Research Techniques Made Simple: Bacterial 16S Ribosomal RNA Gene Sequencing in Cutaneous Research. *The Journal of investigative dermatology*. 2016;136(3): e23–e27. https://doi.org/10.1016/J.JID.2016.01.005.
48. Yue Y, Hu YJ. Extension of PERMANOVA to Testing the Mediation Effect of the Microbiome. *Genes*. 2022;13(6). https://doi.org/10.3390/GENES13060940.
49. Yue Y, Hu YJ. A new approach to testing mediation of the microbiome at both the community and individual taxon levels. *Bioinformatics (Oxford, England)*. 2022;38(12): 3173–3180. https://doi.org/10.1093/bioinformatics/btac310.
50. Jiang Z, He M, Chen J, Zhao N, Zhan X. MiRKAT-MC: A Distance-Based Microbiome Kernel Association Test With Multi-Categorical Outcomes. *Frontiers in genetics*. 2022;13. https://doi.org/10.3389/FGENE.2022.841764.
51. Tzeng J, Lu H, Li WH. Multidimensional scaling for large genomic data sets. *BMC bioinformatics*. 2008;9. https://doi.org/10.1186/1471-2105-9-179.
52. Assarsson E, Lundberg M, Holmquist G, Björkesten J, Thorsen SB, Ekman D, et al. Homogenous 96-plex PEA immunoassay exhibiting high sensitivity, specificity, and excellent scalability. *PloS one*. 2014;9(4). https://doi.org/10.1371/JOURNAL.PONE.0095192.
53. Lundberg M, Thorsen SB, Assarsson E, Villablanca A, Tran B, Gee N, et al. Multiplexed homogeneous proximity ligation assays for high-throughput protein biomarker research in serological material. *Molecular & cellular proteomics : MCP*. 2011;10(4). https://doi.org/10.1074/MCP.M110.004978.
54. Goeman JJ, Van De Geer SA, Van Houwelingen HC. Testing Against a High Dimensional Alternative. *Journal of the Royal Statistical Society Series B: Statistical Methodology*. 2006;68(3): 477–493. https://doi.org/10.1111/J.1467-9868.2006.00551.X.
55. Doncheva NT, Morris JH, Gorodkin J, Jensen LJ. Cytoscape StringApp: Network Analysis and Visualization of Proteomics Data. *Journal of proteome research*. 2019;18(2): 623–632. https://doi.org/10.1021/ACS.JPROTEOME.8B00702.

56. Janssens AS, Pave S, Tensen CP, Teunissen MBM, Out-Luiting JJ, Willemze R, et al. Reduced IL-1Ra/IL-1 ratio in ultraviolet B-exposed skin of patients with polymorphic light eruption. *Experimental Dermatology*. 2009;18(3): 212–217. https://doi.org/10.1111/j.1600-0625.2008.00785.x.
57. Lembo S, Hawk JLM, Murphy GM, Kaneko K, Young AR, McGregor JM, et al. Aberrant gene expression with deficient apoptotic keratinocyte clearance may predispose to polymorphic light eruption. *The British journal of dermatology*. 2017;177(5): 1450–1453. https://doi.org/10.1111/BJD.15200.
58. Van De Pas CB, Kelly DA, Seed PT, Young AR, Hawk JLM, Walker SL. Ultraviolet-Radiation-Induced Erythema and Suppression of Contact Hypersensitivity Responses in Patients with Polymorphic Light Eruption. *Journal of Investigative Dermatology*. 2004;122(2): 295–299. https://doi.org/10.1046/J.0022-202X.2004.22201.X.
59. Hughes AJ, Tawfik SS, Baruah KP, O'Toole EA, O'Shaughnessy RFL. Tape strips in dermatology research. *The British journal of dermatology*. 2021;185(1): 26–35. https://doi.org/10.1111/BJD.19760.
60. Szklarczyk D, Gable AL, Nastou KC, Lyon D, Kirsch R, Pyysalo S, et al. The STRING database in 2021: customizable protein–protein networks, and functional characterization of user-uploaded gene/measurement sets. *Nucleic Acids Research*. 2021;49(D1): D605. https://doi.org/10.1093/NAR/GKAA1074.
61. Wu J, Cotliar R. Afamelanotide: An Orphan Drug with Potential for Broad Dermatologic Applications. *Journal of drugs in dermatology : JDD*. 2021;20(3): 290–294. https://doi.org/10.36849/JDD.5526.
62. Wensink D, Wagenmakers MAEM, Langendonk JG. Afamelanotide for prevention of phototoxicity in erythropoietic protoporphyria. *Expert review of clinical pharmacology*. 2021;14(2): 151–160. https://doi.org/10.1080/17512433.2021.1879638.
63. Patra V, Strobl J, Gruber-Wackernagel A, Vieyra-Garcia P, Stary G, Wolf P. CD11b+ cells markedly express the itch cytokine interleukin-31 in polymorphic light eruption. *The British journal of dermatology*. 2019;181(5): 1079–1081. https://doi.org/10.1111/BJD.18092.
64. Kim HS, Yosipovitch G. The skin microbiota and itch: Is there a link? *Journal of Clinical Medicine*. 2020;9(4). https://doi.org/10.3390/jcm9041190.
65. Nakashima C, Otsuka A, Kabashima K. Interleukin-31 and interleukin-31 receptor: New therapeutic targets for atopic dermatitis. *Experimental Dermatology*. 2018;27(4): 327–331. https://doi.org/10.1111/EXD.13533.
66. Tanew A, Radakovic S, Gonzalez S, Venturini M, Calzavara-Pinton P. Oral administration of a hydrophilic extract of Polypodium leucotomos for the prevention of polymorphic light eruption. *Journal of the American Academy of Dermatology*. 2012;66(1): 58–62. https://doi.org/10.1016/j.jaad.2010.09.773.
67. Patra V, Sérézal IG, Wolf P. Potential of Skin Microbiome, Pro- and/or Pre-Biotics to Affect Local Cutaneous Responses to UV Exposure. *Nutrients*. 2020;12(6): 1–14. https://doi.org/10.3390/NU12061795.
68. Marini A, Jaenicke T, Grether-Beck S, Le Floc'h C, Cheniti A, Piccardi N, et al. Prevention of polymorphic light eruption by oral administration of a nutritional supplement containing lycopene, β-carotene, and Lactobacillus johnsonii: results from a randomized, placebo-controlled, double-blinded study. *Photodermatology, photoimmunology & photomedicine*. 2014;30(4): 189–194. https://doi.org/10.1111/PHPP.12093.

69. Schweintzger NA, Gruber-Wackernagel A, Shirsath N, Quehenberger F, Obermayer-Pietsch B, Wolf P. Influence of the season on vitamin D levels and regulatory T cells in patients with polymorphic light eruption. *Photochemical and Photobiological Sciences*. 2016;15(3): 440–446. https://doi.org/10.1039/C5PP00398A/METRICS.
70. Janssens AS, Pavel S, Out-Luiting JJ, Willemze R, De Gruijl FR. Normalized ultraviolet (UV) induction of Langerhans cell depletion and neutrophil infiltrates after artificial UVB hardening of patients with polymorphic light eruption. *British Journal of Dermatology*. 2005;152(6): 1268–1274. https://doi.org/10.1111/j.1365-2133.2005.06690.x.
71. Schäbitz A, Hillig C, Mubarak M, Jargosch M, Farnoud A, Scala E, et al. Spatial transcriptomics landscape of lesions from non-communicable inflammatory skin diseases. *Nature Communications*. 2022;13(1): 10. https://doi.org/10.1038/S41467-022-35319-W.

Supplementary

CRF: Die Bedeutung des Hautmikrobioms in der Pathophysiologie der Polymorphen Lichtdermatose (Studiencode: PLD-Mikrobiom 2020)

Screening Visite LogNr. des Pat.: .....

Datum: .....

Geburtsdatum des Studienteilnehmers/der Studienteilnehmerin: .....

Patientennummer: (P1, P2, etc.): .....

Spezifische und allgemeine Einschlusskriterien:

☐ PLD ☐ Alter 18-65 Jahre

Allgemeine Ausschlusskriterien:

☐ JA (bitte nachstehend ankreuzen, falls vorliegend)

☐ NEIN (liegen keine vor)

☐ Laufende systemische Therapie mit Steroiden und/oder anderen Immunsuppressiva oder innerhalb der letzten 6 Monate

☐ Systemische antibiotische Therapie in den letzten 6 Wochen

☐ Systemische antientzündliche Therapie (z.B. NSAR) in den letzten 2 Wochen

☐ Lokale antimikrobiell-wirksame Therapie innerhalb der letzten 6 Wochen im Bereich der Hautareale, von denen Abstriche entnommen werden sollen

☐ Allergie auf Klebebänder und/oder Klebestoffe

☐ Schwangerschaft oder Stillperiode

☐ Maligne Hauttumoren bzw. Z.n. malignen Hauttumoren

☐ Autoimmundermatosen (Lupus erythemathodes, Sklerodermie, Dermatomyositis, u.a.)

☐ Photosensitive Erkrankungen (Porphyrie, Xeroderma pigmentosum, u.a.)

☐ Psychiatrische Erkrankungen

☐ Schlechter Allgemeinzustand

Gewicht (kg)	
Körpergröße (cm)	
WHR (Taillenumfang/Hüftumfang)	
Hauttyp	

Unterschrift-Untersucher: .....

Visite 1 (24h vor Beginn der MED-Testung)

Datum: .....

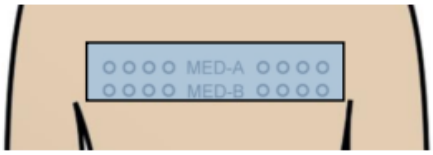

☐Position des MED-Testareals am oberen Rücken festlegen, wie schematisch dargestellt, und markieren (ca. 10 x 30 – 50 cm; über gesamte Breite des Rückens)

☐Obere Reihe (MED-A) des markierten Hautareals mit einem in MED-A Lösung getränkten Tupfer behandeln (60 Sekunden Einwirkzeit)

☐Prozedere für die untere Reihe (MED-B) mit MED-B-Lösung wiederholen

Unterschrift-Untersucher: .....

Visitie 2 (MED-Testung)

Datum: .....

☐Obere Reihe (MED-A) des markierten Hautareals mit einem in MED-A Lösung getränkten Tupfer behandeln (60 Sekunden Einwirkzeit)

☐Prozedere für die untere Reihe (MED-B) mit MED-B-Lösung wiederholen

☐UV-Bestrahlung durchführen

☐Klebestreifenabstriche von MED Testfelder entnehmen

WALDMANN UV801KL (SONNENSIMULATOR)

Abstand von Blaufilter (Soll 15 cm)	
UV6 Intensität (PUVA-Meter)	
UV21 Intensität (PUVA-Meter)	
Nummer des PUVA Meters	
Sunburn MED-Meter	
Durham Thermopile	
Dosis	

UV-EXPOSITION DER TESTFELDER

MED-A	1	2	3	4	5	6
Bestrahlungszeit						
Dosis						

MED-B	1	2	3	4	5	6
Bestrahlungszeit						
Dosis						

Unterschrift-Untersucher: .....

Visite 3 (24h nach MED-Testung)

Datum: .....

☐ Photodokumentation

☐ Visuelle Beurteilung der Hautreaktionen der MED-Testfelder (Erythem und Pigmentierung)

☐ Kolorimetrische Messungen für Erythem/Pigment-Index (je 3 pro Feld)

☐ Messung der Hautqualitäten (TEWL, pH-Wert und Fettgehalt) an den MED-Testfeldern

☐ Hautabstriche von MED-Testfeldern entnehmen

☐ Klebestreifenabstriche von MED-Testfeldern entnehmen

☐ Anwenden der Saugblasen-Methode: 1x Kontrollfeld, 2x minimal-erythematöses Feld (kann ggf. in der oberen/unteren Reihe sub-erythematös imponieren) (simultan an allen 3 Testfelder)

☐ Nadelpunktion des Blasendachs und Aspiration der Blasenflüssigkeit

☐ Abtragen des Blasendachs

☐ Wundauflage

VISUELLES ERYTHEM SCORING DER MED TESTFELDER

	1	2	3	4	5	6
MED-A						
MED-B						
MED-A vs. MED-B						

MED-A vs. MED-B: „=“ (gleich), „>“ (größer) oder „<“ (kleiner)

Grad	**Erythem**
0	kein sichtbares Erythem
0,5	leichtes, inhomogenes Erythem
1	leichtes, homogenes Erythem
2	dunkles Erythem
3	dunkles Erythem mit Ödem
4	dunkles Erythem mit Blasenbildung

VISUELLES PIGMENT SCORING DER MED TESTFELDER

	1	2	3	4	5	6
MED-A						
MED-B						
MED-A vs. MED-B						

MED-A vs. MED-B: „=“ (gleich), „>“ (größer) oder „<“ (kleiner)

Punkte	**Pigmentierung**
0	keine sichtbare Pigmentierung
1	leichte Pigmentierung
2	mäßige Pigmentierung
3	umfangreiche Pigmentierung
4	maximale Pigmentierung

ERYTHEM/PIGMENT-INDEX DER MED-FELDER

MED-A	0 (E/P)	1 (E/P)	2 (E/P)	3 (E/P)	4 (E/P)	5 (E/P)	6 (E/P)
Messung 1	/	/	/	/	/	/	/
Messung 2	/	/	/	/	/	/	/
Messung 3	/	/	/	/	/	/	/

0 = Kontrollfeld

MED-B	0 (E/P)	1 (E/P)	2 (E/P)	3 (E/P)	4 (E/P)	5 (E/P)	6 (E/P)
Messung 1	/	/	/	/	/	/	/
Messung 2	/	/	/	/	/	/	/
Messung 3	/	/	/	/	/	/	/

0 = Kontrollfeld

MESSUNG DER HAUTQUALITÄTEN (TEWL, PH-WERT, FETTGEHALT)

MED-A	0	1	2	3	4	5	6
TEWL (g/h/m²)							
pH-Wert							
Fettgehalt							

MED-B	0	1	2	3	4	5	6
TEWL (g/h/m²)							
pH-Wert							
Fettgehalt							

0 = Kontrollfeld

1. PHOTOPROVOKATION

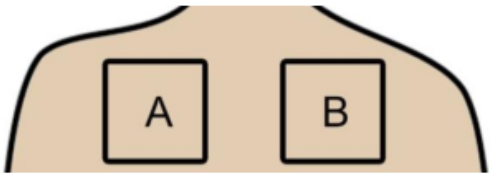

☐ Position von Testfeld A und Testfeld B am oberen Rücken festlegen und markieren

☐ Testfeld A mit einem in Lösung A getränkten Tupfer behandeln (60 Sekunden Einwirkzeit);

☐ Prozedere an Testfeld B mit Lösung B wiederholen

☐ UV-Bestrahlung der Testfelder mit 75% der MED*

☐ Nach 1-2 min Klebestreifenabstriche an den lateralen oberen Ecken entnehmen

☐ Hautabstriche an den lateralen oberen Ecken unterhalb der Klebestreifenabnahmestelle

Anmerkungen: *Falls sich ein unterschiedlicher MED Wert in den MED-Reihen ergeben sollte, wird mit 75% der niedrigeren MED bestrahlt.

MED seitengleich: ☐ JA ☐NEIN

MED-A: …….. **MED-B:** ……

WALDMANN UV801KL (SONNENSIMULATOR)

Abstand von Blaufilter (Soll 15 cm)	
UV6 Intensität (PUVA-Meter)	
UV21 Intensität (PUVA-Meter)	
Nummer des PUVA Meters	
Sunburn MED-Meter	
Durham Thermopile	
Dosis	

UV-EXPOSITION DER TESTFELDER

A	
Bestrahlungszeit	
Dosis	

B	
Bestrahlungszeit	
Dosis	

Unterschrift-Untersucher: ……

Visite 4 (2. Photoprovokation)

Datum: ……

☐Photodokumentation

☐Visuellen Score für Erythem und Pigmentierung bestimmen

☐Reflexionsspektroskopie durchführen (Erythem-Pigment-Index)

☐Klinischen PLD-Score (Betroffenes Areal, Infiltrat, Juckreiz) erheben

☐Messung der Hautqualitäten (TEWL, pH-Wert und Fettgehalt) an den MED-Testfeldern

☐Testfeld A mit einem in Lösung A getränkten Tupfer behandeln (60 Sekunden Einwirkzeit); Prozedere an Testfeld B mit Lösung B wiederholen

☐UV-Bestrahlung der Testfelder mit 0-25% erhöhter Dosis*

☐Nach 1-2 min Klebestreifenabstriche an den inneren, oberen Ecken entnehmen

☐Hautabstriche an den inneren, oberen Ecken unterhalb der Klebestreifenabnahmestelle

Anmerkungen: *Führt die Dosis der vorhergehenden UV-Bestrahlung zu keinem Erythem, erhöht sich die Dosis für die nächste Photoprovokation um maximal 25%. Im Fall eines beobachtbaren Erythems, bleibt die Dosis auf dem jeweiligen Niveau der vorhergehenden Photoprovokation.

VISUELLES ERYTHEM SCORING DER PHOTOPROVOKATION

Grad	0	0,5	1	2	3	4
Links (A)						
Rechts (B)						
A vs. B						

A vs. B: „=" (gleich); „>" (größer) oder „<" (kleiner)

Grad	**Erythem**
0	kein sichtbares Erythem
0,5	leichtes, inhomogenes Erythem
1	leichtes, homogenes Erythem
2	dunkles Erythem
3	dunkles Erythem mit Ödem
4	dunkles Erythem mit Blasenbildung

VISUELLES PIGMENT SCORING DER PHOTOPROVOKATION

Punkte	0	1	2	3	4
Links (A)					
Rechts (B)					
A vs. B					

A vs. B: „=" (gleich); „>" (größer) oder „<" (kleiner)

Punkte	**Pigmentierung**
0	keine sichtbare Pigmentierung
1	leichte Pigmentierung
2	mäßige Pigmentierung
3	umfangreiche Pigmentierung
4	maximale Pigmentierung

ERYTHEM/PIGMENT-INDEX

Links (A)	**(E/P)**
Messung 1	/
Messung 2	/
Messung 3	/

Rechts (B)	**(E/P)**
Messung 1	/
Messung 2	/
Messung 3	/

EFFLORESZENZEN

Links (A)	**Rechts (B)**
☐ makulös	☐ makulös
☐ vesikulär	☐ vesikulär
☐ papulo-vesikulär	☐ papulo-vesikulär
☐ papulös	☐ papulös
☐ plaqueartig	☐ plaqueartig
☐ pruriginös	☐ pruriginös
☐ EEM-artig	☐ EEM-artig

BETROFFENES AREAL

Links (A)	**Rechts (B)**
☐ **0**	☐ **0**
☐ **1** (1 – 24 %)	☐ **1** (1 – 24 %)
☐ **2** (25 – 49 %)	☐ **2** (25 – 49 %)
☐ **3** (50 – 74 %)	☐ **3** (50 – 74 %)
☐ **4** (75 – 100%)	☐ **4** (75 – 100%)

INFILTRATION (Tastbarkeit)

Links (A)	**Rechts (B)**
☐ **0** (keine)	☐ **0** (keine)
☐ **1** (gering)	☐ **1** (gering)
☐ **2** (mäßig)	☐ **2** (mäßig)
☐ **3** (ausgeprägt)	☐ **3** (ausgeprägt)
☐ **4** (maximal)	☐ **4** (maximal)

JUCKREIZ

Links (A)	Rechts (B)
0 – 1 – 2 – 3 – 4 – 5 – 6 – 7 – 8 – 9 – 10	**0 – 1 – 2 – 3 – 4 – 5 – 6 – 7 – 8 – 9 – 10**
□ - □ - □ - □ - □ - □ - □ - □ - □ - □ - □	□ - □ - □ - □ - □ - □ - □ - □ - □ - □ - □

MESSUNG DER HAUTQUALITÄTEN (TEWL, PH-WERT, FETTGEHALT)

A	
TEWL (g/h/m²)	
pH-Wert	
Fettgehalt	

B	
TEWL (g/h/m²)	
pH-Wert	
Fettgehalt	

WALDMANN UV801KL (SONNENSIMULATOR)

Abstand von Blaufilter (Soll 15 cm)	
UV6 Intensität (PUVA-Meter)	
UV21 Intensität (PUVA-Meter)	
Nummer des PUVA Meters	
Sunburn MED-Meter	
Durham Thermopile	
Dosis	

UV-EXPOSITION DER TESTFELDER

A	
Bestrahlungszeit	
Dosis	

B	
Bestrahlungszeit	
Dosis	

Unterschrift-Untersucher: .....

Visite 5 (3. Photoprovokation)

Datum: .....

☐Photodokumentation

☐Visuellen Score für Erythem und Pigmentierung bestimmen

☐Reflexionsspektroskopie durchführen (Erythem-Pigment-Index)

☐Klinischen PLD-Score (Betroffenes Areal, Infiltrat, Juckreiz) erheben

☐Messung der Hautqualitäten (TEWL, pH-Wert und Fettgehalt) an den MED-Testfeldern

☐Testfeld A mit einem in Lösung A getränkten Tupfer behandeln (60 Sekunden Einwirkzeit); Prozedere an Testfeld B mit Lösung B wiederholen

☐UV-Bestrahlung der Testfelder mit 0-25% erhöhter Dosis*

☐Nach 1-2 min Klebestreifen an den unteren, lateralen Ecken entnehmen

☐Hautabstriche an den unteren, lateralen Ecken oberhalb der Klebestreifenabnahmestellen

VISUELLES ERYTHEM SCORING DER PHOTOPROVOKATION

Grad	0	0,5	1	2	3	4
Links (A)						
Rechts (B)						
A vs. B						

A vs. B: „=" (gleich); „>" (größer) oder „<" (kleiner)

Grad	**Erythem**
0	kein sichtbares Erythem
0,5	leichtes, inhomogenes Erythem
1	leichtes, homogenes Erythem
2	dunkles Erythem
3	dunkles Erythem mit Ödem
4	dunkles Erythem mit Blasenbildung

VISUELLES PIGMENT SCORING DER PHOTOPROVOKATION

Punkte	0	1	2	3	4
Links (A)					
Rechts (B)					
A vs. B					

A vs. B: „=" (gleich); „>" (größer) oder „<" (kleiner)

Punkte	**Pigmentierung**
0	keine sichtbare Pigmentierung
1	leichte Pigmentierung
2	mäßige Pigmentierung
3	umfangreiche Pigmentierung
4	maximale Pigmentierung

ERYTHEM/PIGMENT-INDEX

Links (A)	**(E/P)**
Messung 1	/
Messung 2	/
Messung 3	/

Rechts (B)	**(E/P)**
Messung 1	/
Messung 2	/
Messung 3	/

EFFLORESZENZEN

Links (A)	Rechts (B)
☐ makulös	☐ makulös
☐ vesikulär	☐ vesikulär
☐ papulo-vesikulär	☐ papulo-vesikulär
☐ papulös	☐ papulös
☐ plaqueartig	☐ plaqueartig
☐ pruriginös	☐ pruriginös
☐ EEM-artig	☐ EEM-artig

BETROFFENES AREAL

Links (A)	Rechts (B)
☐ **0**	☐ **0**
☐ **1** (1 – 24 %)	☐ **1** (1 – 24 %)
☐ **2** (25 – 49 %)	☐ **2** (25 – 49 %)
☐ **3** (50 – 74 %)	☐ **3** (50 – 74 %)
☐ **4** (75 – 100%)	☐ **4** (75 – 100%)

INFILTRATION (Tastbarkeit)

Links (A)	Rechts (B)
☐ **0** (keine)	☐ **0** (keine)
☐ **1** (gering)	☐ **1** (gering)
☐ **2** (mäßig)	☐ **2** (mäßig)
☐ **3** (ausgeprägt)	☐ **3** (ausgeprägt)
☐ **4** (maximal)	☐ **4** (maximal)

JUCKREIZ

Links (A)	Rechts (B)
0 – 1 – 2 – 3 – 4 – 5 – 6 – 7 – 8 – 9 – 10	**0 – 1 – 2 – 3 – 4 – 5 – 6 – 7 – 8 – 9 – 10**
☐ - ☐ - ☐ - ☐ - ☐ - ☐ - ☐ - ☐ - ☐ - ☐ - ☐	☐ - ☐ - ☐ - ☐ - ☐ - ☐ - ☐ - ☐ - ☐ - ☐ - ☐

MESSUNG DER HAUTQUALITÄTEN (TEWL, PH-WERT, FETTGEHALT)

A	
TEWL (g/h/m²)	
pH-Wert	
Fettgehalt	

B	
TEWL (g/h/m²)	
pH-Wert	
Fettgehalt	

WALDMANN UV801KL (SONNENSIMULATOR)

Abstand von Blaufilter (Soll 15 cm)	
UV6 Intensität (PUVA-Meter)	
UV21 Intensität (PUVA-Meter)	
Nummer des PUVA Meters	
Sunburn MED-Meter	
Durham Thermopile	
Dosis	

UV-EXPOSITION DER TESTFELDER

A	
Bestrahlungszeit	
Dosis	

Unterschrift-Untersucher: .....

Visite 6 (4. Photoprovokation)

Datum: .....

☐ Visuellen Score für Erythem und Pigmentierung bestimmen

☐ Reflexionsspektroskopie durchführen (Erythem-Pigment-Index)

☐ Klinischen PLD-Score (Betroffenes Areal, Infiltrat, Juckreiz) erheben

☐ Messung der Hautqualitäten (TEWL, pH-Wert und Fettgehalt) an den MED-Testfeldern

☐ Testfeld A mit einem in Lösung A getränkten Tupfer behandeln (60 Sekunden Einwirkzeit); Prozedere an Testfeld B mit Lösung B wiederholen

☐ UV-Bestrahlung der Testfelder mit 0-25% erhöhter Dosis*

☐ Nach 1-2 min Klebestreifen an den unteren, inneren Ecken entnehmen

☐ Hautabstriche an den unteren, inneren Ecken oberhalb der Klebestreifenabnahmestellen

☐ Anwenden der Saugblasen-Methode an Testfeld A und B (simultan)

☐ Nadelpunktion des Blasendachs und Aspiration der Blasenflüssigkeit

☐ Abtragen des Blasendachs

☐ Fakultative Stanzbiopsien (Patienteneinverständnis vorausgesetzt) an Testfeldern, bei denen sich klinisch signifikante Unterschiede in den Reaktionen zeigen

☐ Wundversorgung

VISUELLES ERYTHEM SCORING DER PHOTOPROVOKATION

Grad	0	0,5	1	2	3	4
Links (A)						
Rechts (B)						
A vs. B						

A vs. B: „=" (gleich); „>" (größer) oder „<" (kleiner)

Grad	**Erythem**
0	kein sichtbares Erythem
0,5	leichtes, inhomogenes Erythem
1	leichtes, homogenes Erythem
2	dunkles Erythem
3	dunkles Erythem mit Ödem
4	dunkles Erythem mit Blasenbildung

VISUELLES PIGMENT SCORING DER PHOTOPROVOKATION

Punkte	0	1	2	3	4
Links (A)					
Rechts (B)					
A vs. B					

A vs. B: „=" (gleich); „>" (größer) oder „<" (kleiner)

Punkte	Pigmentierung
0	keine sichtbare Pigmentierung
1	leichte Pigmentierung
2	mäßige Pigmentierung
3	umfangreiche Pigmentierung
4	maximale Pigmentierung

ERYTHEM/PIGMENT-INDEX

Links (A)	(E/P)
Messung 1	/
Messung 2	/
Messung 3	/

Rechts (B)	(E/P)
Messung 1	/
Messung 2	/
Messung 3	/

EFFLORESZENZEN

Links (A)	Rechts (B)
☐ makulös	☐ makulös
☐ vesikulär	☐ vesikulär
☐ papulo-vesikulär	☐ papulo-vesikulär
☐ papulös	☐ papulös
☐ plaqueartig	☐ plaqueartig
☐ pruriginös	☐ pruriginös
☐ EEM-artig	☐ EEM-artig

BETROFFENES AREAL

Links (A)	Rechts (B)
☐ **0**	☐ **0**
☐ **1** (1 – 24 %)	☐ **1** (1 – 24 %)
☐ **2** (25 – 49 %)	☐ **2** (25 – 49 %)
☐ **3** (50 – 74 %)	☐ **3** (50 – 74 %)
☐ **4** (75 – 100%)	☐ **4** (75 – 100%)

INFILTRATION (Tastbarkeit)

Links (A)	Rechts (B)
☐ **0** (keine)	☐ **0** (keine)
☐ **1** (gering)	☐ **1** (gering)
☐ **2** (mäßig)	☐ **2** (mäßig)
☐ **3** (ausgeprägt)	☐ **3** (ausgeprägt)
☐ **4** (maximal)	☐ **4** (maximal)

JUCKREIZ

Links (A)	Rechts (B)
0 – 1 – 2 – 3 – 4 – 5 – 6 – 7 – 8 – 9 – 10	**0 – 1 – 2 – 3 – 4 – 5 – 6 – 7 – 8 – 9 – 10**
☐ - ☐ - ☐ - ☐ - ☐ - ☐ - ☐ - ☐ - ☐ - ☐ - ☐	☐ - ☐ - ☐ - ☐ - ☐ - ☐ - ☐ - ☐ - ☐ - ☐ - ☐

MESSUNG DER HAUTQUALITÄTEN (TEWL, PH-WERT, FETTGEHALT)

A	
TEWL (g/h/m²)	
pH-Wert	
Fettgehalt	

B	
TEWL (g/h/m²)	
pH-Wert	
Fettgehalt	

WALDMANN UV801KL (SONNENSIMULATOR)

Abstand von Blaufilter (Soll 15 cm)	
UV6 Intensität (PUVA-Meter)	
UV21 Intensität (PUVA-Meter)	
Nummer des PUVA Meters	
Dosis	

UV-EXPOSITION DER TESTFELDER

A	
Bestrahlungszeit	
Dosis	

B	
Bestrahlungszeit	
Dosis	

FAKULTATIVE STANZBIOPSIE

Stanzbiopsie:

☐ JA ☐ NEIN

Testfeld:

☐ A ☐ B

Studie abgeschlossen:

☐ JA ☐ NEIN

Unterschrift-Untersucher: .....